Scheme 3. Synthesis of Sulfonamide Isosteres with P_1'-Oxazolidinone

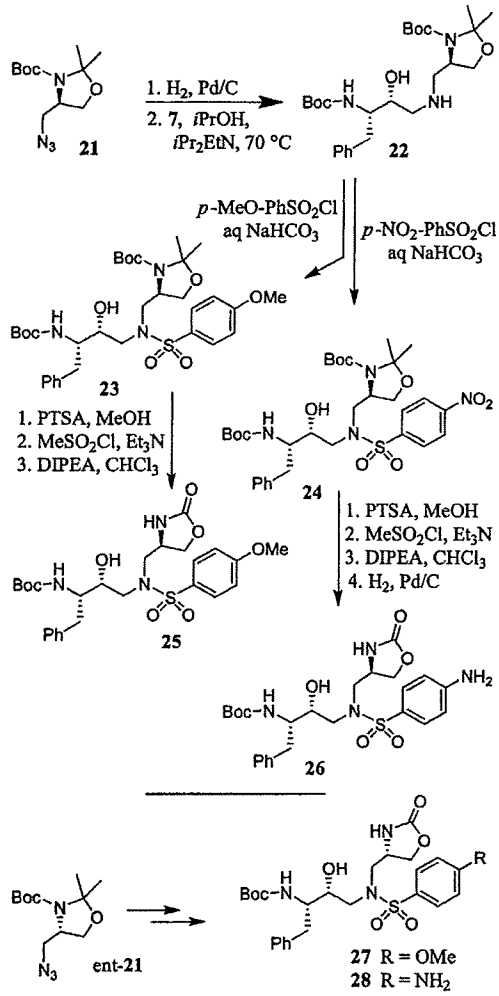

Scheme 4. Synthesis of Oxazolidinone-Derived PIs

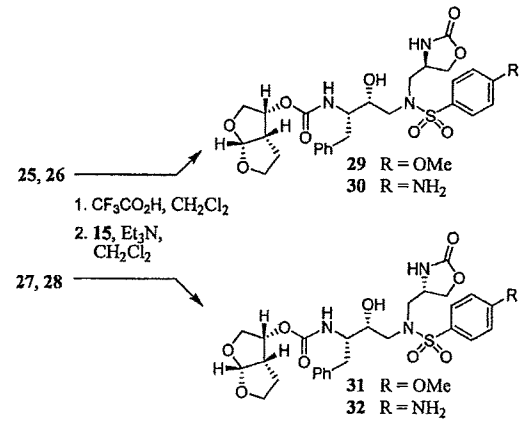

active dimethyloxazolidines **21** and *ent*-**21** were prepared by following the procedure described by Dondini and co-workers.[18] Reduction of these azides by catalytic hydrogenation in methanol afforded the respective amine. Reaction of **21**-derived amine with epoxide **7** in the presence of *i*-Pr_2NEt in 2-propanol afforded amine **22** in 41% yield. Reaction of amine **22** with *p*-methoxybenzenesulfonyl chloride or *p*-nitrobenzenesulfonyl chloride as described previously afforded sulfonamide derivatives **23** and **24** in 80% and 92% yields, respectively. The isopropylidene functionality in **23** and **24** was converted to the corresponding oxazolidinone derivative in a three-step sequence involving (1) treatment of **23** by a catalytic amount of *p*-toluenesulfonic acid (PTSA) in methanol, resulting in the removal of the isopropylidene group, (2) reaction of the resulting Boc-amino alcohol with mesyl chloride in the presence of triethylamine to provide the corresponding mesylate, and (3) treatment of the resulting mesylate with *i*-Pr_2NEt in chloroform at reflux. This has provided oxazolidinone **25** in 45% yield over three steps. The nitrosulfonamide derivative **24** was similarly converted to the corresponding oxazolidinone. Catalytic hydrogenation of the resulting nitro derivative with 10% Pd–C in methanol provided aniline derivative **26** in 37% overall yield over four steps. Enantiomeric azide *ent*-**21** was converted to oxazolidinone derivatives **27** and **28** by following analogous procedures.

The synthesis of inhibitors containing oxazolidinone as P1′-ligand and bis-THF as the P2-ligand is shown in Scheme 4. Treatment of oxazolidinones **25**–**28** with 30% CF_3CO_2H in CH_2Cl_2 at 23 °C afforded the corresponding amines. Reaction of the resulting amines with activated mixed carbonate **15** in the presence of Et_3N in CH_2Cl_2 afforded the target inhibitors **29**–**32** in excellent yields (80–90%). The structures of these inhibitors are shown in Table 1.

Results and Discussion

Our examination of the X-ray structure of **1**-bound HIV-1 protease and its respective modeling initially suggested that a methyl-2-pyrrolidinone may interact well with residues in the S1′-site.[15] As shown in Table 1, our first set of inhibitors contain a (*R*)-hydroxyethylamine sulfonamide isostere with either the bis-THF or Cp-THF as the P2-ligand and *p*-methoxysulfonamide or *p*-aminosulfonamide as the P2′-ligand. The enzyme inhibitory potency of these PIs was evaluated according to the procedure reported by Toth and Marshall.[19] Inhibitor **17a** with (*S*)-methyl-2-pyrrolidinone displayed an enzyme K_i of 1 nM. Inhibitor **17b** with a Cp-THF showed a 3-fold improvement of potency. Antiviral activity of these inhibitors was determined in MT-2 human T-lymphoid cells exposed to HIV-1_{LAI}. Interestingly, both inhibitors have shown dramatic reduction in antiviral activity. Inhibitors **17a** and **17b** have shown IC_{50} values of 0.48 and 0.23 μM, respectively. However, these inhibitors are significantly less potent compared to inhibitors with an isobutyl group as the P1′-ligand.[7c,9] Incorporation of *p*-aminosulfonamide (PIs **18a** and **18b**) as the P2′-ligand led to a drop in enzyme inhibitory as well as antiviral potency. Inhibitor **19a** containing (*R*)-methyl-2-pyrrolidinone as the P1′-ligand has shown 10-fold enhancement of enzyme K_i over the (*S*)-isomer **17a**. It showed a slight improvement in antiviral activity compared to inhibitor **17a**. Inhibitor **19b** with (*R*)-methyl-2-pyrrolidinone as the P1′-ligand and Cp-THF as the P2-ligand resulted in the most potent inhibitor in the series. It has shown an enzymatic K_i of 99 pM and a 10-fold improvement (IC_{50} = 0.026 μM) in antiviral activity relative to epimeric (*S*)-pyrrolidinone derivative **17b**, suggesting an important role for the P1′-ring stereochemistry. Indeed, an X-ray structure of **19b**-bound HIV-1 protease revealed that the pyrrolidinone carbonyl and the NH functionalities were positioned to hydrogen-bond with residues in the S1′-site. Interestingly, the combination of P1′-methylpyrrolidi-

Table 1. Enzymatic Inhibitory Activity of Lactam and Oxazolidinone Containing Inhibitors[b]

Entry	Inhibitor	K_i(nM)	IC_{50}(nM)[a]
1.	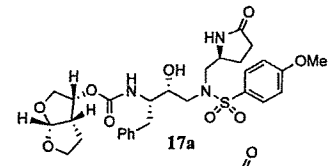 **17a**	0.85±0.02	0.48±0.05
2.	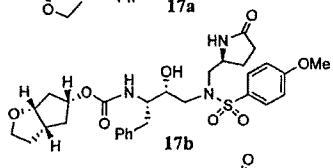 **17b**	0.31±0.03	0.23±0.08
3.	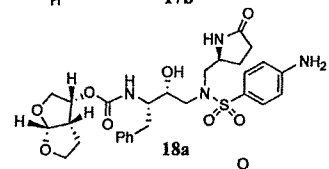 **18a**	0.28±0.03	>1
4.	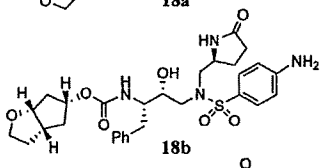 **18b**	1.27±0.15	>1
5.	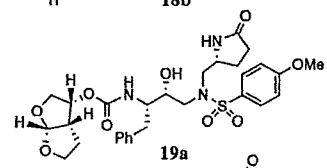 **19a**	0.12±0.003	0.25±0.11
6.	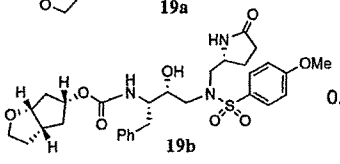 **19b**	0.099±0.003	0.026±0.002
7.	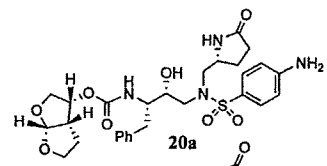 **20a**	0.85±0.2	>1
8.	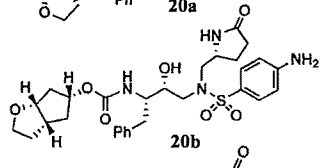 **20b**	0.31±0.03	0.60±0.24
9.	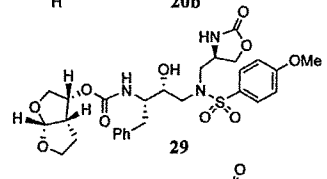 **29**	0.28±0.03	0.48±0.17
10.	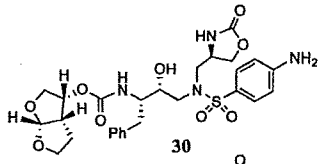 **30**	0.31±0.03	>1
11.	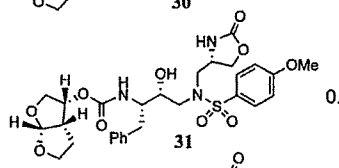 **31**	0.035±0.01	0.31±0.21
12.	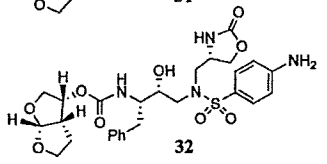 **32**	0.24±0.03	>1

[a] Values are the mean of at least two experiments. [b] Human T-lymphoid (MT-2) cells (2×10^3) were exposed to 100 $TCID_{50}$ values of HIV-1_{LAI} and cultured in the presence of each PI, and IC_{50} values were determined using the MTT assay. The IC_{50} values of amprenavir (APV), saquinavir (SQV), and indinavir (IDV) were 0.03, 0.015, and 0.03 μM, respectively.

none and polar P2′-*p*-aminosulfonamide led to PIs with subnanomolar enzyme activity. However, antiviral activity was reduced drastically. In PIs **29**–**32**, we have incorporated both (*S*)- and (*R*)-oxazolidinone derivatives as substitutes for the respective pyrrolidinone isomers. As can be seen, oxazolidinone derivatives **29**–**32** have shown subnanomolar enzyme inhibitory potency. Inhibitors with *p*-methoxysulfonamide as the P2′-ligand displayed comparable antiviral activity relative to pyrrolidinone derivatives. Consistent with stereochemical preference, the (*R*)-oxazolidinone with *p*-methoxysulfonamide has shown better enzyme K_i values. However, the antiviral activity of these compounds is very similar. In general, both pyrrolidinone and oxazolidinone functionalities appear to be nicely accommodated in the S1′-site.

While inhibitor **31** is very potent in enzyme inhibitory assay, the significant reduction of antiviral potency is possibly due to poor cellular permeability of this polar functionality. Inhibitor **19b** appeared to be most potent among the series of inhibitors examined. It exhibited comparable antiviral activity with the FDA approved PIs amprenavir, saquinavir, and indinavir in the same assay.

Inhibitor **19b** was subsequently examined for its activity against a clinical wild-type X_4-HIV-1 isolate (HIV-$1_{ERS104pre}$) along with various multidrug-resistant clinical X_4- and R_5-HIV-1 isolates using PBMCs as target cells.[8b] As can be seen in Table 2, the potency of **19b** against HIV-$1_{ER104pre}$ (IC_{50} = 28 nM) was comparable to FDA approved PIs indinavir, amprenavir, and lopinavir with IC_{50} values of 28, 25, and 30 nM, respectively. Darunavir, on the other hand, is nearly 10-fold more potent (IC_{50} = 3.6 nM) than **19b** and the above-mentioned PIs. Interestingly, of all the PIs tested, indinavir was least able to suppress the replication of the multidrug-resistant clinical isolate examined (HIV-$1_{MDR/MM}$, HIV-$1_{MDR/TM}$, HIV-$1_{MDR/C}$, and HIV-$1_{MDR/G}$) with IC_{50} values greater than 1 μM. Both amprenavir and lopinavir displayed 10-fold or greater reduction in potency except against HIV-1MDR/G, where lopinavir showed a 5-fold reduction in potency. A more detailed virologic study using inhibitor **19b** will be published elsewhere.[20] Darunavir has maintained impressive activity against all the multidrug-resistant variants. Inhibitor **19b**, while less potent than darunavir, maintained near full potency against multidrug-resistant clinical isolates examined. This impressive drug-resistance property of **19b** is possibly due to its extensive interactions, particularly its ability to make extensive hydrogen bonding throughout the active site of the protease's backbone. Furthermore, inhibitor **19b** blocked the infection and replication

Table 2. Anti-HIV Activity of **19b** against Selected Clinical Isolates Highly Resistant to Multiple Protease Inhibitors[a]

		EC_{50} (μM)				
virus	phenotype	IDV	APV	LPV	DRV	**19b**
HIV-$1_{ERS104pre}$ (wild-type)	X4	0.028 ± 0.005	0.025 ± 0.006	0.03 ± 0.001	0.0036 ± 0.0002	0.028 ± 0.004
HIV-1_{TM} (MDR)	X4	>1 (>36)	0.25 ± 0.02 (10)	0.73 ± 0.53 (24)	0.0036 ± 0.0002 (1)	0.029 ± 0.004 (1)
HIV-1_{MM} (MDR)	R5	>1 (>36)	0.32 ± 0.03 (13)	0.72 ± 0.31 (24)	0.019 ± 0.009 (5)	0.042 ± 0.002 (2)
HIV-1_C (MDR)	X4	>1 (>36)	0.35 ± 0.03 (14)	0.32 ± 0.01 (11)	0.015 ± 0.001 (4)	0.023 ± 0.007 (1)
HIV-1_G (MDR)	X4	0.29 ± 0.07 (10)	0.33 ± 0.16 (13)	0.14 ± 0.01 (5)	0.014 ± 0.006 (4)	0.027 ± 0.001 (1)

[a] Amino acid substitutions identified in the protease-encoding regions of HIV-$1_{ERS104pre}$, HIV-1_{TM}, HIV-1_{MM}, HIV-1_C, and HIV-1_G compared to the consensus B sequence cited from the Los Alamos data base include L63P, L10I/K14R/R41K/M46L/I54V/L63P/A71V/V82A/L90M/I93L, L10I/K43T/M46L/I54V/L63P/A71V/V82A/L90M/Q92K, L10I/I15V/K20R/L24I/M36I/M46L/I54V/I62V/L63P/K70Q/V82A/L89M, and L10I/V11I/T12E/I15V/L19I/R41K/M46L/L63P/A71T/V82A/L90M, respectively. The EC_{50} values were determined by employing PHA-PBM as target cells and the inhibition of p24 *Gag* protein production as an end point. All values were determined in duplicate or triplicate, and those shown are derived from the results of three independent experiments. Numbers in parentheses represent fold changes of EC_{50} values against each isolate compared to EC_{50} values against HIV-$1_{ERS104pre}$. MDR: multidrug-resistant.

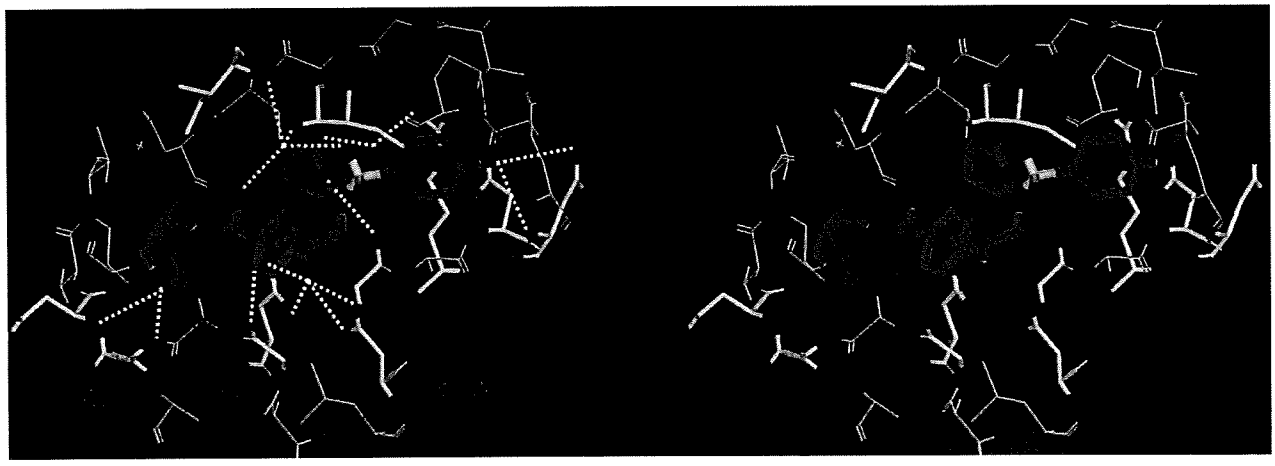

Figure 2. Stereoview of the major conformation of the X-ray structure of inhibitor **19b**-bound HIV-1 protease.

of each of the HIV-1_{NL4-3} variants exposed to and selected by up to 5 μM saquinavir, amprenavir, indinavir, nelfinavir, or ritonavir and a 1 μM lopinavir or atazanavir with EC_{50} values ranging from 0.036 to 0.14 μM.[20]

X-ray Crystallography. The binding mode of inhibitor **19b** was determined from the X-ray crystal structure of its complex with wild-type HIV-1 protease. The crystal structure was solved and refined at 1.29 Å resolution with an *R* factor of 14.1%. In this high resolution structure, the inhibitor was bound to the HIV-1 protease active site in two orientations with the relative occupancy of 0.8/0.2. The protease dimer comprises residues 1−99 and 1′−99′ of the two subunits, and the inhibitor binding site is formed by both subunits. The P1′-pyrrolidine ring also showed two alternative conformations with equal occupancy and related by about 18° rotation around the C12−C13 bond. A stereoview of the major conformation is shown in Figure 2 (only one conformation is shown for P1′). As shown, extensive interactions from P2 to P2′ were observed between the inhibitor and the protease active site, most notably favorable polar interactions including hydrogen bonds, weaker C−H···O and C−H···π interactions. The isostere hydroxyl group forms asymmetric hydrogen bonds to the carboxylate oxygen atoms of the catalytic Asp25 and Asp25′ with distances of 2.4−3.3 Å. Also, four direct hydrogen bonds are formed between the oxygens or nitrogens of the inhibitor atoms and the protease backbone atoms. These include cyclic ether oxygen of the P2-Cp-THF and the Asp-29 NH, the urethane NH with the carbonyl oxygen of Gly-27, P2′-methoxy oxygen and Asp-30′ NH. One conformation of the P1′-pyrrolidinone formed a hydrogen bond between the NH and the carbonyl oxygen of Gly-27′ and a water-mediated hydrogen bond between the P1′-pyrrolidinone

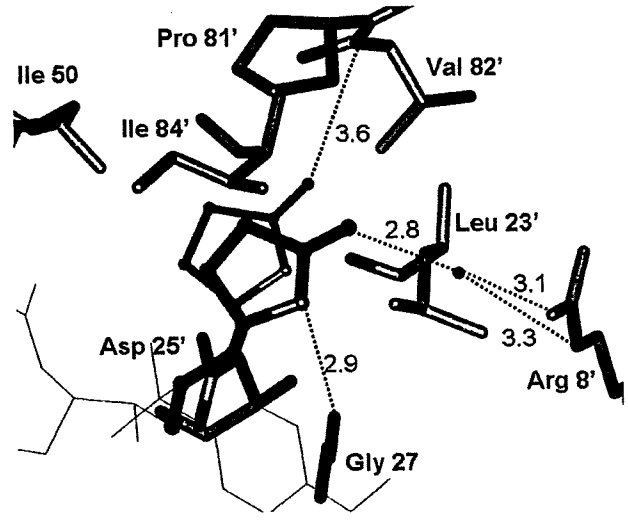

Figure 3. Protease interactions with the two alternate conformations of the inhibitor's pyrrolidine ring. The inhibitor is in green with thick bonds for the major and thin bonds for the minor conformations of the pyrrolidine ring. Hydrogen bonds are shown as dotted lines. Distances between donor and acceptor atoms are shown in Å.

carbonyl and the side chain of Arg-8. The other conformation of the P1′ group formed hydrophobic and C−H···O interactions with Pro-81′ and Val-82′, as shown in Figure 3. Also, there exists a tetracoordinated water-mediated interaction where the amides of Ile50 and Ile50′ donate hydrogen bonds, and the inhibitor's urethane carbonyl and one of the sulfonamide oxygen

accept hydrogen bonds from the water molecule. These interactions are conserved in a majority of other HIV-1 protease complexes with inhibitors[21] or substrate analogues.[22]

The weaker polar interactions such as C−H···O and water−π interactions can be analyzed accurately in this high resolution structure.[23,24] These interactions are important for inhibitor-protease binding and must be considered in the design of inhibitors. The C−H···O interactions of the inhibitor with the carbonyl oxygens of Gly-48, Gly-48′, and Gly-27′ mimic the conserved hydrogen bonds observed with peptide analogue structures.[21,22] A conserved water−π interaction is observed between the P2′ aromatic ring of the inhibitor and the amide of Asp29′, which is similar to the interaction with darunavir and other structure-based designed PIs from our laboratories.[25,26] The bigger polar P1′ group of the 2-pyrrolidinone ring in inhibitor **19b** instead of the isobutyl group in PI's **1** and **2** introduces a new direct hydrogen bond with the backbone of HIV-1 protease and one new water-mediated hydrogen bond between the inhibitor and the side chain residue of the protease. The two alternative conformations of the P1′ group with occupancy of 0.5/0.5 provide more flexible binding within the S1′ subsite, which is likely to enhance the inhibition of resistant proteases.

As mentioned earlier, inhibitor **19b** maintained near full potency against multidrug-resistant clinical isolates examined. On the other hand, **19b** is less potent than darunavir possibly due to the bigger and less optimum size of the P1′-ligand. The design strategy of incorporating new polar interactions with conserved backbone regions of the protease warrants further investigation in light of the current molecular insight into these ligand-binding site interactions.

Conclusion

We have designed a number of HIV-1 protease inhibitors with methyl-2-pyrrolidinone and methyloxazolidinone as the P1′-ligand to enhance hydrogen bonding with the protein backbone atoms in the S1′-subsite. The ligands were synthesized in enantiomerically pure forms, and a series of inhibitors were prepared and evaluated in combination with P2-bis-THF and P2-Cp-THF ligands. In general, these inhibitors exhibited enzyme inhibitory activity lower than the corresponding inhibitors with a P1′-isobutyl group. Our SAR studies indicated the importance of ligand stereochemistry and also preference for the P2-Cp-THF ligand. Interestingly, the polar P1′-ligand influenced their cellular properties. The inhibitors exhibited reduction in antiviral activity possibly due to changes in the molecule's overall lipophilicity. Our investigation resulted in the identification of inhibitor **19b** which has displayed similar antiviral potency as the other FDA approved inhibitors such as indinavir, lopinavir, and amprenavir. Inhibitor **19b**, however, is nearly 10-fold less potent than darunavir. Of particular importance, **19b** has maintained full potency against the examined panel of multidrug-resistant HIV-1 variants. A high resolution X-ray structure of **19b**-bound HIV-1 protease revealed a new hydrogen bonding of the P1′-pyrrolidinone NH with the backbone carbonyl of Gly27′. Also, there is a water mediated hydrogen bond with the pyrrolidinone carboxyl and Arg8′ side chain. Furthermore, the P1′-pyrrolidinone showed two alternative conformations that filled the S1′ subsite. These new interactions and the conformational flexibility most likely contributed to its impressive properties against multidrug-resistant clinical variants. Further investigations including optimization of ligand-binding properties are in progress.

Experimental Section

General. All moisture sensitive reactions were carried out under nitrogen or argon atmosphere. Anhydrous solvents were obtained as follows: THF, diethyl ether, and benzene, distilled from sodium and benzophenone; dichloromethane, pyridine, triethylamine, and diisopropylethylamine, distilled from CaH_2. All other solvents were HPLC grade. Silica gel column chromatography was performed with Whatman 240−400 mesh silica gel under low pressure. TLC was carried out with E. Merck silica gel 60-F-254 plates. ^1H and ^{13}C NMR spectra were recorded on Varian Mercury 300 and Bruker Avance 400 and 500 spectrometers. Optical rotations were measured using a Perkin-Elmer 341 polarimeter.

(*S*)-5-(Aminomethyl)-2-pyrrolidinone 6. To a stirred solution of (*S*)-5-(hydroxymethyl)-2-pyrrolidinone **4** (300 mg, 2.61 mmol) and *p*-toluenesulfonyl chloride (646 mg, 3.34 mmol) in CH_2Cl_2 (6 mL) at 0 °C was added DMAP (64 mg, 0.52 mmol) and Et_3N (472 μL, 3.34 mmol). The resulting mixture was allowed to warm to 23 °C and stirred for 12 h. The reaction was then quenched with 7 mL of water, and the aqueous layer was extracted with CH_2Cl_2. The combined organic extracts were washed with 1 N HCl and dried over anhydrous Na_2SO_4. Removal of solvent under reduced pressure followed by flash chromatography purification (100% EtOAc as the eluent) yielded (*S*)-toluenesulfonate **5** ((0.7 g, 93%) as a yellowish solid. R_f = 0.50 (5% MeOH in $CHCl_3$); ^1H NMR (400 MHz, $CDCl_3$) δ 1.75−1.80 (m, 1H), 2.19−2.35 (m, 3H), 2.44 (s, 3H), 3.85−3.92 (m, 2H), 4.00−4.03 (m, 1H), 6.49 (s, 1H), 7.35 (d, 2H, J = 8.0 Hz), 7.77 (d, 2H, J = 8.1 Hz); ^{13}C NMR (100 MHz, $CDCl_3$) δ 21.6, 22.7, 29.2, 52.5, 71.9, 121.9, 130.0, 132.3, 145.3, 178.2.

To a stirred solution of the above tosylate (638 mg, 2.37 mmol) in DMF (20 mL) was added NaN_3 (462 mg, 2.37 mmol). The resulting solution was stirred at 55 °C for 9 h. Removal of solvent under reduced pressure followed by flash chromatography purification (6% MeOH in $CHCl_3$ as the eluent) provided the (*S*)-azidopyrrolidinone (330 mg, 99%) as a yellow oil. R_f = 0.50 (10% MeOH in $CHCl_3$); ^1H NMR (400 MHz, $CDCl_3$) δ 1.76−1.84 (m, 1H), 2.18−2.44 (m, 3H), 3.28 (dd, 1H, J = 6.5, 12.2 Hz), 3.43 (dd, 1H, J = 4.6, 12.3 Hz), 3.77−3.83 (m, 1H), 7.38 (s, 1H); ^{13}C NMR (100 MHz, $CDCl_3$) δ 23.9, 29.7, 53.6, 55.8, 178.7.

To a solution of the above azide (125 mg, 0.89 mmol) in EtOAc (10 mL) was added Pd/C (15 mg). The mixture was stirred at 23 °C under a hydrogen filled balloon for 4 h, then filtered over Celite, and the filter cake was washed with EtOAc and MeOH. Removal of solvent under reduced pressure followed by flash chromatography purification (5% MeOH in $CHCl_3$ as the eluent) afforded the corresponding (*S*)-amine **6** (105 mg, quantitive) as a yellow oil. R_f = 0.05 (20% MeOH in $CHCl_3$); ^1H NMR (400 MHz, $CDCl_3$) δ 1.41 (brs 2H), 1.56−1.65 (m, 1H), 2.01−2.12 (m, 1H), 2.19−2.24 (m, 2H), 2.52 (dd, 1H, J = 7.5, 12.8 Hz), 2.69 (dd, 1H, J = 4.3, 12.9 Hz), 3.50−3.57 (m, 1H), 7.90 (brs, 1H); ^{13}C NMR (100 MHz, $CDCl_3$) δ 24.0, 30.2, 47.3, 57.1, 179.0.

***tert*-Butyl-(2*R*,3*R*)-3-hydroxy-4-[((*S*)-5-oxopyrrolidin-2-yl)-methylamino]-1-phenylbutan-2-yl-carbamate 8.** To a solution of amine **6** (107 mg, 0.94 mmol) in *i*-PrOH (5 mL) were added *tert*-butyl-[*S*-(*R*,*R*)]-(-)-(1-oxiranyl-2-phenylethyl)carbamate **7** (62 mg, 0.23 mmol) and DIPEA (204 μL, 1.2 mmol). The resultant mixture was stirred at 65 °C for 18 h and then concentrated under reduced pressure. Flash chromatography purification (15% MeOH in $CHCl_3$ as the eluent) yielded title compound **8** (76 mg, 85%). R_f = 0.47 (25% MeOH in $CHCl_3$); ^1H NMR (400 MHz, $CDCl_3$) δ 1.30 (s, 9H), 1.62−1.71 (m, 1H), 2.13−2.18 (m, 1H), 2.30−2.32 (m, 2 H), 2.52 (d, 1H, J = 8.86 Hz), 2.64−2.73 (m, 4H), 2.96 (d, 1H, J = 9.8 Hz), 3.54 (s, 1H), 3.72−3.75 (m, 4H), 4.99 (brs, 1H), 7.15−7.26 (m, 5H), 8.02 (s, 1H); ^{13}C NMR (100 MHz, $CDCl_3$) δ 24.6, 28.3, 30.2, 36.3, 51.7, 54.0, 54.4, 55.3, 71.5, 79.2, 126.2, 128.2, 129.4, 138.1, 155.9, 178.9; LRMS-ESI (*m*/*z*) $[M + Na]^+$ 400.

***tert*-Butyl-(2*R*,3*R*)-3-hydroxy-4-(4-methoxy-*N*-(((*S*)-5-oxopyrrolidin-2-yl)methyl)phenylsulfonamido)-1-phenylbutan-2-ylcarbamate 9.** To a stirred solution of amine **8** (22 mg, 0.06 mmol) in CH_2Cl_2 (3 mL) and aqueous saturated $NaHCO_3$ (3 mL) was added 4-methoxybenzenesulfonyl chloride (35.6 mg, 0.17 mmol). This reaction mixture was stirred for 12 h followed by extraction of the aqueous layer with CH_2Cl_2; the combined organic extracts were dried over anhydrous Na_2SO_4. Removal of solvent under reduced pressure followed by flash chromatography purification (6% MeOH in $CHCl_3$ as the eluent) provided compound **9** (31 mg, quantitative). R_f = 0.40 (10% MeOH in $CHCl_3$); ^{1}H NMR (500 MHz, $CDCl_3$) δ 1.28 (s, 9H), 1.54−1.62 (m, 1H), 2.14−2.21 (m, 1H), 2.32−2.35 (m, 2H), 2.68−2.75 (m, 2H), 2.72 (s, 3H), 2.81−2.88 (m, 2H), 2.97−3.03 (m, 3H), 3.64−3.72 (m, 1H), 4.01−4.05 (m, 1H), 5.06 (d, 1H, J = 8.9 Hz), 6.93 (d, 2H, J = 8.6 Hz), 7.16−7.19 (m, 3H), 7.27−7.28 (m, 3H), 7.61 (d, 2H, J = 8.5 Hz); ^{13}C NMR (125 MHz, $CDCl_3$) δ 23.9, 28.1, 29.6, 29.9, 36.1, 53.4, 53.9, 54.5, 55.5, 56.0, 71.9, 79.5, 114.3, 126.3, 126.3, 129.3, 129.5, 137.7, 155.9, 163.1, 178.4; LRMS-ESI (*m/z*) $[M + Na]^+$ 570.

***tert*-Butyl-(2*R*,3*R*)-4-(4-Cbz-amino-*N*-(((*S*)-5-oxopyrrolidin-2-yl)methyl)phenylsulfonamido)-3-hydroxy-1-phenylbutan-2-ylcarbamate 10.** To a stirred solution of amine **8** (93.6 mg, 0.25 mmol) in CH_2Cl_2 (10 mL) and aqueous saturated $NaHCO_3$ (10 mL) was added 4-nitrobenzenesulfonyl chloride (60 mg, 0.27 mmol). This reaction mixture was stirred for 7 h followed by extraction of the aqueous layer with CH_2Cl_2; the combined organic extracts were dried over anhydrous Na_2SO_4. Removal of solvent under reduced pressure followed by flash chromatography purification (dry transfer, 8% MeOH in $CHCl_3$ as the eluent) provided (*S*)-nitrosulfonamide (112 mg, 80%) as a yellowish solid. R_f = 0.56 (10% MeOH in $CHCl_3$).

The above nitrosulfone (103 mg, 0.18 mmol) was dissolved in EtOAc (20 mL), and Pd/C (11 mg) was added. The mixture was stirred under a hydrogen filled balloon for 8 h at 23 °C. It was then filtered over Celite, and the filter cake was washed with EtOAc and MeOH. Removal of solvent under reduced pressure followed by flash chromatography purification (2.5% MeOH in $CHCl_3$ as the eluent) afforded the corresponding (*S*)-amine (77 mg, 79%) as a white solid. R_f = 0.26 (5% MeOH in $CHCl_3$); ^{1}H NMR (500 MHz, $CDCl_3$) 1.35 (s, 9H), 1.59−1.57 (m, 1H), 2.15−2.23 (m, 1H), 2.29−2.42 (m, 2H), 2.82−2.87 (m, 3H), 3.02 (dd, 1H, J = 4.75, 14.0), 3.13 (dd, 1H, J = 10, 13.2 Hz), 3.30 (dd, 2H, J = 1.8, 14.4 Hz), 3.73−3.82 (m, 1H), 3.90−3.95 (m, 1H), 3.99 (d, 1H, J = 6.2 Hz), 4.72 (d, 1H, J = 8.2 Hz), 6.72 (d, 2H, J = 7.9 Hz), 7.20−7.32 (m, 5H), 7.37 (s, 1H), 7.57 (d, 2H, J = 8.2 Hz); ^{13}C NMR (125 MHz, $CDCl_3$) δ 24.3, 28.6, 30.0, 36.5, 53.6, 54.4, 54.9, 56.6, 72.6, 79.8, 114.4, 125.0, 126.7, 128.7, 129.9, 130.0, 138.3, 151.5.

To a stirred solution of the above amine (33.1 mg, 0.06 mmol) in CH_2Cl_2 (3 mL) was added pyridine (30 μL, 0.37 mmol) and benzyl chloroformate (20 μL, 0.137 mmol). This reaction mixture was stirred for 3 h, then quenched with 5 drops of benzylamine followed by removal of solvent under reduced pressure. Column chromatography over silica gel (2.5% MeOH in $CHCl_3$ as the eluent) provided (*S*)-Cbz-amine **10** (41 mg, 99%) as a white solid. R_f = 0.37 (5% MeOH in $CHCl_3$); ^{1}H NMR (500 MHz, $CDCl_3$) δ 1.56 (brs, 1H), 2.12−2.18 (m, 1H), 2.26−2.41 (m, 2H), 2.71−2.78 (m, 2H), 2.79−89 (m, 1H), 3.02 (dd, 1H, J = 8.2, 18.0 Hz), 3.19−3.26 (m, 1H), 3.38 (d, 1H, J = 14.4 Hz), 3.77 (brs, 1H), 3.94−3.99 (m, 2H), 4.73 (d, 1H, J = 8.5 Hz), 5.21 (s, 2H), 7.19−7.22 (m, 3H), 7.25−7.29 (m, 3H), 7.31−7.39 (m, 4H), 7.57 (d, 2H, J = 7.6 Hz), 7.69 (d, 2H, J = 7.7 Hz); ^{13}C NMR (125 MHz, $CDCl_3$) δ 24.1, 28.7, 30.1, 36.6, 53.3, 54.3, 54.8, 56.8, 67.7, 72.6, 80.0, 118.6, 126.8, 128.7, 128.8, 128.9, 129.0, 129.4, 129.9, 131.6, 136.0, 138.1, 143.0, 153.3, 156.3, 178.9; LRMS-ESI (*m/z*) $[M + Na]^+$ 689.

***tert*-Butyl-(2*R*,3*R*)-3-hydroxy-4-(4-methoxy-*N*-(((*R*)-5-oxopyrrolidin-2-yl)methyl)phenylsulfonamido)-1-phenylbutan-2-ylcarbamate 11.** To a stirred solution of (*R*)-5-(hydroxymethyl)-2-pyrrolidinone *ent*-**5** (500 mg, 4.34 mmol) and *p*-toluenesulfonyl chloride (1.08 g, 5.6 mmol) in CH_2Cl_2 (10 mL) at 0 °C were added DMAP (106 mg, 0.87 mmol) and Et_3N (780 μL, 5.6 mmol). The resulting mixture was allowed to warm to 23 °C and stirred for 12 h. The reaction was then quenched with 10 mL of water, and the aqueous layer was extracted with CH_2Cl_2. The combined organic extracts were washed with 1 N HCl and dried over anhydrous Na_2SO_4. Removal of solvent under reduced pressure followed by flash chromatography (2.5% MeOH in $CHCl_3$ as the eluent) yielded the (*R*)-toluenesulfonate (1.8 g, 93%) as a yellowish solid. R_f = 0.50 (5% MeOH in $CHCl_3$); ^{1}H NMR (400 MHz, $CDCl_3$) δ 1.70−1.79 (m, 1H), 2.13−2.35 (m, 3H), 2.42 (s, 3H), 3.84−3.89 (m, 2H), 3.96−3.04 (m, 1H), 6.76 (s, 1H), 7.33 (d, 2H, J = 8.04 Hz), 7.76 (d, 2H, J = 8.2 Hz); ^{13}C NMR (100 MHz, $CDCl_3$) δ 21.6, 22.7, 29.3, 52.6, 71.9, 127.9, 130.0, 132.3, 145.3, 178.1.

To a stirred solution of the above toluenesulfonate (1.08 g, 4.03 mmol) in DMF (30 mL) was added NaN_3 (1.31 g, 20.2 mmol). The resulting solution was stirred at 55 °C for 12 h. Solvent was then removed under reduced pressure followed by flash chromatography purification (6% MeOH in $CHCl_3$ as the eluent), providing the (*R*)-azidopyrrolidinone (558 mg, 99%) as a yellow oil. R_f = 0.44 (5% MeOH in $CHCl_3$); ^{1}H NMR (500 MHz, $CDCl_3$) δ 1.72−1.79 (m, 1H), 2.13−2.37 (m, 3H), 3.22 (dd, 1H, J = 6.3, 12.3 Hz), 3.37 (dd, 1H, J = 4.7, 12.3 Hz), 3.72−3.78 (m, 1H), 7.69 (s, 1H); ^{13}C NMR (125 MHz, $CDCl_3$) δ 24.3, 30.2, 54.1, 56.1, 179.3.

To a solution of the above azide (528 mg, 3.77 mmol) in EtOAc (35 mL) was added Pd/C (40 mg). The mixture was stirred at 23 °C under a hydrogen filled balloon for 4 h, then filtered over Celite, and the filter cake was washed with EtOAc and MeOH. Removal of solvent under reduced pressure followed by flash chromatography purification (5% MeOH in $CHCl_3$ as the eluent) afforded the (*R*)-amine *ent*-**6** (257 mg, 95%) as a yellow oil. R_f = 0.05 (20% MeOH in $CHCl_3$); ^{1}H NMR (400 MHz, $CDCl_3$) δ 1.59−1.69 (m, 1H), 2.06−2.15 (m, 1H), 2.23−2.30 (m, 4H), 2.57 (dd, 1H, J = 7.6, 12.8 Hz), 2.74 (dd, 1H, J = 4.1, 12.9 Hz), 3.56−3.65 (m, 1H), 7.80 (brs, 1H); ^{13}C NMR (100 MHz, $CDCl_3$) δ 24.1, 30.2, 47.1, 56.8, 179.0.

To a solution of amine *ent*-**6** (430 mg, 3.76 mmol) in *i*-PrOH (20 mL) were added *tert*-butyl-[*S*-(*R*,*R*)]-(−)-(1-oxiranyl-2-phenylethyl)carbamate **7** (250 mg, 0.94 mmol) and *i*-Pr_2EtN (1.5 mL, 8.6 mmol). The resultant mixture was stirred at 65 °C for 36 h and then concentrated under reduced pressure. Flash chromatography purification (10% MeOH in $CHCl_3$ as the eluent) yielded the (*R*)-hydroxylamine (**8***R*) (300 mg, 84%). R_f = 0.33 (20% MeOH in $CHCl_3$); ^{1}H NMR (400 MHz, $CDCl_3$) δ 1.33 (s, 9H), 1.64−1.73 (m, 1H), 2.13−2.22 (m, 1H), 2.28−2.34 (m, 2 H), 2.54 (dd, 1H, J = 9.0, 11.8 Hz), 2.65 (dd, 1H, J = 7.2, 13.2 Hz), 2.73−2.85 (m, 4H), 2.94 (dd, 1H, J = 4.4, 14.0 Hz), 3.43 (s, 1H), 3.51−3.60 (m, 1H), 3.70−3.76 (m, 1H), 3.79−3.84 (m, 1H), 5.02 (d, 1H, J = 8.9 Hz), 7.16−7.27 (m, 5H), 7.94 (s, 1H); ^{13}C NMR (100 MHz, $CDCl_3$) δ 24.6, 28.3, 30.2, 36.3, 52.1, 54.2, 54.6, 55.4, 71.6, 79.2, 126.2, 128.3, 129.4, 138.1, 155.9, 178.9; LRMS-ESI (*m/z*) $[M + Na]^+$ 400.

To a stirred solution of above (*R*)-hydroxylamine (**8***R*) (40 mg, 0.105 mmol) in CH_2Cl_2 (4 mL) and aqueous saturated $NaHCO_3$ (4 mL) was added 4-methoxybenzenesulfonyl chloride (66 mg, 0.318 mmol). This reaction mixture was stirred for 12 h followed by extraction of the aqueous layer with CH_2Cl_2; the combined organic extracts were dried over anhydrous Na_2SO_4. Removal of solvent under reduced pressure followed by flash chromatography purification (4% MeOH in $CHCl_3$ as the eluent) provided compound **11** (54 mg, 93%). R_f = 0.40 (10% MeOH in $CHCl_3$); ^{1}H NMR (400 MHz, $CDCl_3$) δ 1.32 (s, 9H), 1.64−1.68 (m, 1H), 2.17−2.21 (m, 2H), 2.34−2.40 (m, 2H), 2.76−2.84 (m, 1H), 2.91−3.06 (m, 3H), 3.16−3.29 (m, 2H), 3.75−3.80 (m, 1H), 3.84 (s, 3H), 3.96−4.02 (m, 2H), 4.99 (d, 1H, J = 8.7 Hz), 6.95 (d, 2H, J = 8.8 Hz), 7.16−7.28 (m, 5H), 7.68 (d, 2H, J = 8.8 Hz), 7.93 (s, 1H); ^{13}C NMR (100 MHz, $CDCl_3$) δ 24.4, 28.2, 29.9, 35.7, 35.4, 54.7, 55.2, 55.6, 55.8, 57.8, 73.9, 79.5, 114.4, 126.2, 128.3, 129.3, 129.5, 138.0, 155.9, 163.1, 178.6; LRMS-ESI (*m/z*) $[M + Na]^+$ 670.

tert*-Butyl-(2*R*,3*R*)-4-(4-Cbz-amino-*N*-(((*R*)-5-oxopyrrolidin-2-yl)methyl)phenylsulfonamido)-3-hydroxy-1-phenylbutan-2-yl-carbamate 12.** To a stirred solution of (*R*)-hydroxylamine (**8R*) (116 mg, 0.3 mmol) in CH_2Cl_2 (10 mL) and aqueous saturated $NaHCO_3$ (10 mL) was added 4-nitrobenzenesulfonyl chloride (74 mg, 0.33 mmol). This reaction mixture was stirred for 12 h followed by extraction of the aqueous layer with CH_2Cl_2; the combined organic extracts were dried over anhydrous Na_2SO_4. Removal of solvent under reduced pressure followed by flash chromatography purification (dry transfer, 5% MeOH in $CHCl_3$ as the eluent) provided the (*R*)-nitrosulfonamide (164 mg, 96%) as a yellowish solid. $R_f = 0.56$ (10% MeOH in $CHCl_3$).

The above nitrosulfonamide (154 mg, 0.27 mmol) was redisolved in EtOAc (25 mL) and treated with Pd/C (16 mg) under argon. Argon was then replaced with a hydrogen filled balloon, and the mixture was allowed to stir for 12 h at 23 °C. It was then filtered over Celite, and the filter cake was washed with EtOAc and MeOH. Removal of solvent under reduced pressure followed by flash chromatography purification (6% MeOH in $CHCl_3$ as the eluent) afforded the corresponding (*R*)-aniline (123 mg, 83%) as an amorphous solid. $R_f = 0.45$ (10% MeOH in $CHCl_3$); ^{1}H NMR (500 MHz, $CDCl_3$) δ 1.31 (s, 9H), 1.58−1.64 (m, 1H), 2.15−2.21 (m, 1H), 2.29 (t, 2H, J = 8.2 Hz), 2.73−2.86 (m, 3H), 2.99 (dd, 1H, J = 4.4, 13.9 Hz), 3.23 (d, 1H, J = 13.8 Hz), 3.30 (d, 1H, J = 14.8 Hz), 3.74 (brs, 1H), 3.92 (brs, 1H), 3.99 (d, 1H, J = 5.7), 4.31 (s, 1H), 5.01 (d, 1H, J = 9.1 Hz), 6.63 (d, 2H, J = 8.5 Hz), 7.16−7.21 (m, 3H), 7.24−7.27 (m, 2H), 7.48 (d, 2H, J = 8.5 Hz); ^{13}C NMR (125 MHz, $CDCl_3$) δ 24.3, 28.1, 29.8, 35.5, 54.6, 55.0, 55.5, 57.7, 73.8, 79.5, 113.9, 125.0, 126.2, 128.2, 129.3, 129.4, 137.8, 151.0, 155.9, 178.2; LRMS-ESI (*m*/*z*) $[M + Na]^+$ 555.

To a stirred solution of the above (*R*)-aniline (101 mg, 0.19 mmol) in CH_2Cl_2 (15 mL) was added pyridine (34 μL, 0.41 mmol) and benzyl chloroformate (60 μL, 0.41 mmol). This reaction mixture was stirred for 1.5 h, then quenched with 3 drops of benzylamine, followed by removal of solvent under reduced pressure. Column chromatography over silica gel (6% MeOH in $CHCl_3$ as the eluent) provided the (*R*)-Cbz-amine **12** (120 mg, 95%) as a white solid. R_f = 0.35 (10% MeOH in $CHCl_3$); ^{1}H NMR (500 MHz, $CDCl_3$) δ 1.29 (s, 9H), 1.55−1.65 (m, 1H), 2.15−2.23 (m, 1H), 2.26−2.31 (m, 2H), 2.60−2.75 (m, 3H), 2.97 (dd, 1H, J = 8.2, 18.1 Hz), 3.29 (d, 1H, J = 17.7 Hz), 3.36 (dd, 1H, J = 2.4, 14.9 Hz), 3.64 (s, 1H), 3.88−3.92 (m, 1H), 3.98−4.02 (m, 1H), 5.12 (d, 1H, J = 9.0 Hz), 5.17 (s, 2H), 7.14−7.19 (m, 3H), 7.21−7.28 (m, 3H), 7.30−7.37 (m, 4H), 7.54 (d, 2H, J = 8.6 Hz), 7.63 (d, 2H, J = 8.8); ^{13}C NMR (125 MHz, $CDCl_3$) δ 24.8, 28.6, 30.2, 36.0, 55.1, 55.8, 55.9, 58.2, 67.6, 74.4, 80.0, 118.6, 126.7, 128.6, 128.7, 128.8, 129.0, 129.0, 129.7, 130.3, 131.2, 136.1, 138.2, 143.4, 153.6, 178.9; LRMS-ESI (*m*/*z*) $[M + Na]^+$ 689.

(3*R*,3a*S*,6a*R*)-Hexahydrofuro[2,3-*b*]furan-3-yl(2*S*,3*R*)-3-hydroxy-4-(4-methoxy-*N*-(((*S*)-5-oxopyrrolidin-2-yl)methyl)phenylsulfonamido)-1-phenylbutan-2-ylcarbamate 17a. A solution of compound **9** (10 mg, 0.02 mmol) in 30% trifluoroacetic acid (in CH_2Cl_2, 3 mL) was stirred 23 °C for 40 min, then concentrated under reduced pressure to give the crude amine **13***S*. This residue was redissolved in CH_2Cl_2 (3 mL), treated with Et_3N (20 μL, 0.13 mmol), followed by carbonate **15** (5.5 mg, 0.02 mmol) and stirred at 23 °C for 12 h. The reaction mixture was then concentrated under reduced pressure, and the residue was purified by flash chromatography (2% MeOH in $CHCl_3$ as the eluent) to give inhibitor **17a** (11.3 mg, 98%) as a white solid. $R_f = 0.48$ (10% MeOH in $CHCl_3$); ^{1}H NMR (500 MHz, $CDCl_3$) δ 1.48 (dd, 1H, J = 5.5, 13.2 Hz), 1.58−1.68 (m, 2H), 2.17−2.26 (m, 1H), 2.34−2.49 (m, 2H), 2.76 (dd, 1H, J = 9.8, 14.0 Hz), 2.85−2.95 (m, 3H), 3.10−3.16 (m, 2H), 3.22 (dd, 1H, (dd, 1H, J = 9.9, 13.7 Hz), 3.67−3.74 (m, 2H), 3.82−3.85 (dt, 1H, J = 1.8, 8.4 Hz), 3.87 (s, 3H), 3.94 (dd, 1H, J = 6.2, 9.6 Hz), 3.96−4.01 (m, 1H), 4.04−4.08 (m, 1H), 5.0 (q, 1H, J = 6.1, 7.9 Hz), 5.64 (d, 1H, J = 5.2 Hz), 6.98 (d, 2H, J = 8.9 Hz), 7.19−7.29 (m, 3H), 7.26−7.29 (m, 2H), 7.58 (brs, 1H), 7.69 (d, 2H, J = 8.8 Hz); ^{13}C NMR (125 MHz, $CDCl_3$) δ 23.9, 25.7, 29.5, 35.9, 45.2, 53.4, 53.9, 55.1, 55.6, 56.4, 69.5, 70.8, 72.3, 73.3, 109.2, 114.4, 126.4, 128.3, 128.6, 129.2, 129.4, 137.6, 155.4, 163.2, 178.5. LRMS-ESI (*m*/*z*) $[M + H]^+$ 604.2; HRMS-ESI (*m*/*z*) $[M + H]^+$ calcd for $C_{29}H_{38}N_3O_9S$ 604.2329, found 604.2332.

(3a*S*,5*R*,6a*R*)-Hexahydro-2*H*-cyclopenta[*b*]furan-5-yl-(2*S*,3*R*)-3-hydroxy-4-(4-methoxy-*N*-(((*S*)-5-oxopyrrolidin-2-yl)methyl)phenylsulfonamido)-1-phenylbutan-2-ylcarbamate 17b. A solution of compound **9** (11.8 mg, 0.02 mmol) in 30% trifluoroacetic acid (in CH_2Cl_2, 1.5 mL) was stirred at 23 °C for 40 min, then concentrated under reduced pressure to give the crude amine **13***S*. This crude residue was redissolved in CH_2Cl_2 (1.5 mL), treated with Et_3N (63 μL, 0.45 mmol), followed by carbonate **16** (6.4 mg, 0.02 mmol), and stirred at 23 °C for 6 h. The reaction mixture was then concentrated under reduced pressure and the residue was purified by flash chromatography (1% MeOH in $CHCl_3$ as the eluent) to give inhibitor **17b** (11.5 mg, 87%) as a white solid. R_f = 0.35 (5% MeOH in $CHCl_3$); ^{1}H NMR (500 MHz, $CDCl_3$) δ 1.45 (d, 1H, J = 14.3 Hz), 1.55−1.59 (m, 1H), 1.88 (d, 1H, J = 15.1 Hz), 1.95−2.06 (m, 3H), 2.17−2.24 (m, 1H), 2.33−2.48 (m, 2H), 2.60−2.67 (m, 1H), 2.78 (dd, 1H, J = 9.1, 14.1 Hz), 2.88−2.97 (m, 2H), 3.09 (dd, 1H, J = 4.3, 14.1 Hz), 3.12−3.18 (m, 2H), 3.64−3.68 (m, 1H), 3.82−3.85 (m, 2H), 3.86 (s, 3H), 3.89−3.95 (m, 1H), 3.99−4.05 (m, 1H), 4.39−4.42 (m, 1H), 4.69 (d, 1H, J = 4.1 Hz), 4.87−4.90 (m, 1H), 4.91 (d, 1H, J = 8.9 Hz), 6.98 (d, 2H, J = 8.9 Hz), 7.20−7.23 (m, 3H), 7.27−7.30 (m, 2H), 7.42 (s, 1H), 7.70 (d, 2H, J = 8.9 Hz); ^{13}C NMR (125 MHz, $CDCl_3$) δ 24.0, 29.8, 33.8, 35.9, 38.3, 39.4, 41.5, 53.2, 53.3, 53.9, 54.8, 55.5, 56.3, 67.6, 72.2, 83.7, 114.3, 126.4, 128.4, 128.7, 129.3, 129.5, 137.5, 156.1, 163.1, 178.3. LRMS-ESI (*m*/*z*) $[M + Na]^+$ 624.0; HRMS-ESI (*m*/*z*) $[M + Na]^+$ calcd for $C_{30}H_{39}N_3NaO_8S$ 624.2356, found 624.2352.

(3*R*,3a*S*,6a*R*)-Hexahydrofuro[2,3-*b*]furan-3-yl(2*S*,3*R*)-4-(4-amino-*N*-(((*S*)-5-oxopyrrolidin-2-yl)methyl)phenylsulfonamido)-3-hydroxy-1-phenylbutan-2-ylcarbamate 18a. The Cbz-protected amine **10** (31 mg, 0.04 mmol) was treated with 30% trifluoroacetic acid in CH_2Cl_2 (6 mL) and stirred at 23 °C for 40 min, then concentrated under reduced pressure to give the crude amine **14***S*. This residue was redissolved in CH_2Cl_2 (6 mL), charged with Et_3N (64 μL, 0.46 mmol), followed by carbonate **15** (14 mg, 0.05 mmol), and stirred at 23 °C for 12 h. Reaction was quenched with 3 drops of benzylamine and concentrated under reduced pressure. Flash chromatography purification (4% MeOH in $CHCl_3$ as the eluent) provided the Cbz-protected inhibitor (23 mg, 86%) as a white solid. $R_f = 0.46$ (10% MeOH in $CHCl_3$).

To the above Cbz-protected inhibitor (13.3 mg, 0.018 mmol), in EtOAc (6 mL) under argon, was added Pd/C (3 mg). The mixture was stirred at 23 °C under a hydrogen filled balloon for 3 h, then filtered over Celite, and the filter cake was washed with EtOAc and MeOH. Removal of solvent under reduced pressure followed by flash chromatography purification (3% MeOH in $CHCl_3$ as the eluent) provided the title inhibitor **18a** (7.4 mg, 68%) as a white solid. $R_f = 0.19$ (5% MeOH in $CHCl_3$); ^{1}H NMR (500 MHz, $CDCl_3$) δ 1.44 (d, 1H, J = 5.4 Hz), 1.59−1.69 (m, 2H), 2.16−2.25 (m, 1H), 2.36 (t, 2H, J = 7.9 Hz), 2.68 (dd, 1H, J = 9.8, 13.9 Hz), 2.85−2.95 (m, 3H), 3.03−3.09 (m, 2H), 3.13 (dd, 1H, J = 4.4, 14.1 Hz), 3.67−3.72 (m, 2H), 3.79−3.89 (m, 3H), 3.93 (dd, 1H, J = 6.0, 9.7 Hz), 4.01−4.06 (m, 1H), 4.96 (q, 1H, J = 5.9, 7.9 Hz), 5.63 (d, 1H, J = 5.1 Hz), 6.72 (d, 2H, J = 8.2 Hz), 7.17−7.21 (m, 3H), 7.24−7.28 (m, 2H), 7.50 (d, 2H, J = 8.4 Hz); ^{13}C NMR (125 MHz, $CDCl_3$) δ 24.3, 26.2, 30.0, 36.6, 45.8, 53.6, 54.2, 55.6, 56.6, 70.0, 71.5, 72.7, 73.6, 109.7, 114.6, 124.9, 126.8, 128.8, 129.7, 129.9, 130.3, 151.4, 155.9, 178.3. LRMS-ESI (*m*/*z*) $[M + H]^+$ 589.2; HRMS-ESI (*m*/*z*) $[M + H]^+$ calcd for $C_{28}H_{37}N_4O_8S$ 589.2332, found 589.2336.

(3a*S*,5*R*,6a*R*)-Hexahydro-2*H*-cyclopenta[*b*]furan-5-yl-(2*S*,3*R*)-4-(4-amino-*N*-(((*S*)-5-oxopyrrolidin-2-yl)methyl)phenylsulfonamido)-3-hydroxy-1-phenylbutan-2-ylcarbamate 18b. The Cbz-protected amine **10** (29.6 mg, 0.04 mmol) was treated with 30% trifluoroacetic acid (in CH_2Cl_2, 6 mL) and stirred at 23 °C for 40 min, then concentrated under reduced pressure to give the crude amine **14***S*. The residue was redissolved in CH_2Cl_2 (6 mL), charged with Et_3N (31 μL, 0.22 mmol), followed by carbonate **16** (13.1 mg, 0.05 mmol), and stirred at 23 °C for 4 h. Reaction was

quenched with 2 drops of benzylamine and concentrated under reduced pressure. Flash chromatography purification (4% MeOH in $CHCl_3$ as the eluent) provided the Cbz-protected inhibitor (26.1 mg, 82%) as a white solid. $R_f = 0.49$ (10% MeOH in $CHCl_3$).

To a solution of the above protected inhibitor (17 mg, 0.02 mmol), in EtOAc (5 mL) under argon, was added Pd/C (3 mg). The mixture was stirred at 23 °C under a H_2 filled balloon for 5 h, then filtered over Celite, and the filter cake was washed with EtOAc and MeOH. Removal of solvent under reduced pressure, followed by flash chromatography purification (5% MeOH in $CHCl_3$ as the eluent) provided inhibitor **18b** (14 mg, 75%) as a white solid. R_f = 0.27 (10% MeOH in $CHCl_3$); ^{1}H NMR (500 MHz, $CDCl_3$) δ 1.41−1.45 (m, 1H), 1.56−1.67 (m, 3H), 1.85 (d, 1H, J = 13.4 Hz), 1.96−2.04 (m, 3H), 2.14−2.21 (m, 1H), 2.31−2.42 (m, 2H), 2.61 (brs, 1H), 2.74−2.85 (m, 3H), 3.09 (dd, 1H, J = 4.4, 14.4 Hz), 3.15−3.20 (m, 1H), 3.25 (d,1H, J = 14.3 Hz), 3.66−3.70 (q, 1H, J = 7.1, 7.4 Hz), 3.83−3.88 (m, 2H), 3.91−3.96 (m, 1H), 3.96−4.25 (m, 1H), 4.40 (t, 1H, J = 5.9 Hz), 4.87 (brs, 1H), 4.93 (d, 1H, J = 8.9 Hz), 6.69 (d, 2H), 7.18−7.22 (m, 3H), 7.28−7.30 (m, 2H), 7.55 (d, 2H, J = 8.4 Hz), 7.63 (s, 1H); ^{13}C NMR (125 MHz, $CDCl_3$) δ 24.3, 30.1, 34.1, 36.7, 38.7, 39.8, 41.9, 53.5, 54.3, 55.3, 56.8, 68.0, 72.8, 84.1, 114.6, 125.3, 126.8, 128.8, 129.9, 130.1, 138.1, 151.4, 156.6, 178.9. LRMS-ESI (m/z) [M + H]$^+$ 586.9; HRMS-ESI (m/z) [M + H]$^+$ calcd for $C_{29}H_{39}N_4O_7S$ 587.2539, found 587.2539.

(3*R*,3a*S*,6a*R*)-Hexahydrofuro[2,3-*b*]furan-3-yl-(2*S*,3*R*)-3-hydroxy-4-(4-methoxy-*N*-(((*R*)-5-oxopyrrolidin-2-yl)methyl)phenylsulfonamido)-1-phenylbutan-2ylcarbamate 19a. A solution of compound **11** (20 mg, 0.03 mmol) in 30% trifluoroacetic acid (in CH_2Cl_2, 3 mL) was stirred 23 °C for 40 min, then concentrated under reduced pressure. The residue was redissolved in CH_2Cl_2 (3 mL), treated with Et_3N (51 μL, 0.36 mmol), followed by carbonate **15** (11 mg, 0.04 mmol), and stirred at 23 °C for 12 h. The reaction mixture was then concentrated under reduced pressure and the residue was purified by flash chromatography (2% MeOH in $CHCl_3$ as the eluent) to give inhibitor **19a** (21 mg, 92%) as a white solid. R_f = 0.41 (10% MeOH in $CHCl_3$); ^{1}H NMR (500 MHz, $CDCl_3$) δ 1.44 (dd, 1H, J = 5.6, 13.2 Hz), 1.57−1.67 (m, 2H), 1.81−1.91 (m, 1H), 2.19−2.27 (m, 1H), 2.33−2.41 (m, 2H), 2.73 (dd, 1H J = 10.35, 13.9 Hz), 2.83−2.91 (m, 2H), 2.95 (dd, 1H, J = 8.9, 14.9 Hz), 3.11 (dd, 1H, J = 4.2, 14.0 Hz), 3.26−3.30 (ddd, 2H, J = 2.6, 7.0, 14.3 Hz), 3.64−3.70 (m, 1H), 3.74 (dd, 1H, J = 5.5, 9.8 Hz), 3.76−3.81 (dt, 1H, J = 1.62, 8.0 Hz), 3.87 (s, 3H), 3.89−3.93 (q, 1H, J = 4.0, 5.6 Hz), 4.03−4.06 (m, 2H), 4.98−5.02 (q, 1H, J = 5.65, 7.9 Hz), 5.62 (d, 1H, J = 5.4 Hz), 6.98 (d, 2H, J = 8.9 Hz), 7.17−7.27 (m, 5H), 7.70 (d, 2H, J = 8.8 Hz), 7.89 (s, 1H); ^{13}C NMR (125 MHz, $CDCl_3$) δ 24.2, 25.7, 29.8, 35.4, 45.4, 55.0, 55.3, 55.5, 55.7, 58.1, 69.5, 71.0, 73.3, 74.0, 109.2, 114.4, 126.3, 128.3, 128.8, 129.2, 129.4, 137.8, 155.5, 163.2, 178.5. LRMS-ESI (m/z) [M + Na]$^+$ 626.3; HRMS-ESI (m/z) [M + Na]$^+$ calcd for $C_{29}H_{37}N_3$ Na O_9S 626.2148, found 626.2156.

(3a*S*,5*R*,6a*R*)-Hexahydro-2*H*-cyclopenta[*b*]furan-5-yl-(2*S*,3*R*)-3-hydroxy-4-(4-methoxy-*N*-(((*R*)-5-oxopyrrolidin-2-yl)methyl)phenylsulfonamido)-1-phenylbutan-2-ylcarbamate 19b. A solution of compound **11** (21 mg, 0.04 mmol) in 30% trifluoroacetic acid (in CH_2Cl_2, 3 mL) was stirred at 23 °C for 40 min, then concentrated under reduced pressure. The residue was redissolved in CH_2Cl_2 (3 mL), treated with Et_3N (27 μL, 0.19 mmol), followed by carbonate **16** (12 mg, 0.04 mmol), and stirred at 23 °C for 12 h. The reaction mixture was then concentrated under reduced pressure and the residue was purified by flash chromatography (1% MeOH in $CHCl_3$ as the eluent) to give inhibitor **19b** (21 mg, 93%) as a white solid. R_f = 0.31 (5% MeOH in $CHCl_3$); ^{1}H NMR (500 MHz, $CDCl_3$) δ 1.48 (d, 1H, J = 14.1 Hz), 1.58−1.62 (m, 1H), 1.83−2.04 (m, 5H), 2.19−2.25 (m, 1H), 2.31−2.41 (m, 2H), 2.59−2.67 (m, 1H), 2.73 (dd, 1H, J = 9.0, 13.9 Hz), 3.03 (dd, 1H, J = 7.0, 15.0 Hz), 3.08−3.16 (m, 2H), 3.19 (d, 1H, J = 14.9 Hz), 3.57−3.63 (m, 1H), 3.83−3.86 (m, 3H), 3.86 (s, 3H), 3.94−3.99 (m, 1H), 4.78 (d, 1H, J = 13.7 Hz), 4.90 (s, 1H), 5.36 (d, 1H, J = 8.1 Hz), 6.97 (d, 2H, J = 8.6 Hz), 7.18−7.28 (m, 5H), 7.46 (d, 1H, J = 18.4 Hz), 7.70 (d, 2H, J = 8.8 Hz); ^{13}C NMR (125 MHz, $CDCl_3$) δ 22.5, 30.0, 31.4, 33.9, 35.8, 38.2, 39.5, 41.7, 54.6, 54.9, 55.5, 56.0, 57.7, 67.7, 74.0, 83.9, 114.4, 126.2, 128.2, 128.9, 129.3, 129.4, 137.9, 156.1, 163.1, 178.5. LRMS-ESI (m/z) [M + H]$^+$ 601.7; HRMS-ESI (m/z) [M + H]$^+$ calcd for $C_{30}H_{40}N_3O_8S$ 602.2536, found 602.2536.

(3*R*,3a*S*,6a*R*)-Hexahydrofuro[2,3-*b*]furan-3-yl-(2*S*,3*R*)-4-(4-amino-*N*-(((*R*)-5-oxopyrrolidin-2-yl)methyl)phenylsulfonamido)-3-hydroxy-1-phenylbutan-2-ylcarbamate 20a. A solution of the (*R*)-aniline **12** (15 mg, 0.03 mmol) in 30% trifluoroacetic acid (in CH_2Cl_2, 3 mL) was stirred at 23 °C for 40 min, then concentrated under reduced pressure. The residue was redissolved in CH_2Cl_2 (3 mL), treated with Et_3N (40 μL, 0.28 mmol), followed by carbonate **15** (9.2 mg, 0.03 mmol), and stirred at 23 °C for 6 h. The reaction mixture was then concentrated under reduced pressure and the residue was purified by flash chromatography (4% MeOH in $CHCl_3$ as the eluent) to give inhibitor **20a** (12.5 mg, 75%) as a white solid. R_f = 0.26 (10% MeOH in $CHCl_3$); ^{1}H NMR (500 MHz, $CDCl_3$) δ 1.35 (dd, 1H, J = 5.7 Hz), 1.50−1.63 (m, 2H), 2.15−2.23 (m, 1H), 2.27−2.31 (m, 2H), 2.56−2.72 (m, 3H), 2.82−2.87 (m, 2H), 3.07 (dd, 1H, J = 4.0, 14.0 Hz), 3.36 (q, 1H, J = 1.4, 3.5 Hz), 3.36 (q, 1H, J = 2.0, 3.4 Hz), 3.60−3.65 (m, 1H), 3.70 (dd, 1H, J = 5.4, 9.8 Hz), 3.75−3.79 (dt, 1H, J = 1.96, 8.3 Hz), 3.80−3.86 (m, 1H), 3.88 (dd, 1H, J = 5.9, 9.8 Hz), 3.90−3.94 (m, 1H), 3.99−4.02 (m, 1H), 4.92−4.97 (q, 1H, J = 5.7, 8.1 Hz), 5.58 (d, 1H, J = 5.8 Hz), 5.92 (d, 1H, J = 9.5 Hz), 6.63 (d, 2H, J = 8.7 Hz), 7.13−7.22 (m, 5H), 7.46 (d, 2H, J = 8.7 Hz); ^{13}C NMR (125 MHz, $CDCl_3$) δ 24.1, 25.7, 29.7, 35.3, 45.4, 55.0, 55.5, 55.6, 58.1, 69.5, 71.0, 73.1, 73.9, 109.2, 113.8, 124.2, 126.2, 128.2, 129.1, 129.3, 137.8, 151.4, 155.6, 178.6. LRMS-ESI (m/z) [M + Na]$^+$ 611.4; HRMS-ESI (m/z) [M + Na]$^+$ calcd for $C_{28}H_{36}N_4NaO_8S$ 611.2152, found 611.2149.

(3a*S*,5*R*,6a*R*)-Hexahydro-2*H*-cyclopenta[*b*]furan-5-yl-(2*S*,3*R*)-4-(4-amino-*N*-(((*R*)-5-oxopyrrolidin-2-yl)methyl)phenylsulfonamido)-3-hydroxy-1-phenylbutan-2-ylcarbamate 20b. The Cbz-amine **12** (40 mg, 0.06 mmol) was treated with 30% trifluoroacetic acid (in CH_2Cl_2, 6 mL) and stirred at 23 °C for 40 min, then concentrated under reduced pressure. This residue was redissolved in CH_2Cl_2 (6 mL), charged with Et_3N (42 μL, 0.3 mmol), followed by carbonate **16** (19 mg, 0.07 mmol), and stirred at 23 °C for 12 h. Reaction was quenched with 3 drops of benzylamine and concentrated under reduced pressure. Flash chromatography purification (5% MeOH in $CHCl_3$ as the eluent) provided the Cbz-protected inhibitor (32.1 mg, 75%) as a white solid. R_f = 0.41 (10% MeOH in $CHCl_3$).

To the above Cbz-protected inhibitor (25.8 mg, 0.03 mmol), in EtOAc (5 mL) under argon, was added Pd/C (5 mg). The mixture was stirred at 23 °C under a hydrogen filled balloon for 3 h, then filtered over Celite, and the filter cake was washed with EtOAc and MeOH. Removal of solvent under reduced pressure followed by flash chromatography purification (7.5% MeOH in $CHCl_3$ as the eluent) provided the title inhibitor **20b** (16.2 mg, 77%) as a white solid. R_f = 0.51 (15% MeOH in $CHCl_3$); ^{1}H NMR (500 MHz, $CDCl_3$) δ 1.46 (m, 1H), 1.58−1.64 (m, 1H), 1.77−1.84 (m, 1H), 1.86−2.04 (m, 5H), 2.15−2.23 (m, 1H), 2.32−2.36 (m, 2H), 2.59−2.65 (m, 1H), 2.68 (dd, 1H, J = 9.2, 14.0 Hz), 2.95−3.04 (m, 2H), 3.11 (d, 2H, J = 13.7 Hz), 3.18 (d, 1H, J = 14.9 Hz), 3.57−3.62 (q, 1H, J = 6.9, 7.7 Hz), 3.82−3.87 (q, 2H, J = 6.5, 7.9 Hz), 3.92−3.97 (m, 1H), 4.30 (s, 2H), 4.37 (t, 1H, J = 5.7 Hz), 4.75 (s, 1H), 4.89 (s, 1H), 5.40 (d, 1H, J = 8.4 Hz), 6.66 (d, 2H, J = 8.6 Hz), 7.16−7.22 (m, 3H), 7.24−7.27 (m, 2H), 7.40 (s, 1H), 7.51 (d, 2H, J = 8.6 Hz); ^{13}C NMR (125 MHz, $CDCl_3$) δ 23.7, 30.0, 33.9, 35.9, 38.1, 39.5, 41.7, 54.6, 54.8, 55.9, 57.6, 67.7, 74.0, 76.6, 84.0, 114.1, 124.9, 126.2, 128.2, 129.3, 129.4, 137.9, 151.0, 156.2, 178.4. LRMS-ESI (m/z) [M + Na]$^+$ 609.0; HRMS-ESI (m/z) [M + Na]$^+$ calcd for $C_{29}H_{38}N_4NaO_7S$ 609.2359, found 609.2362.

(*R*)-*tert*-Butyl-4-(((2*R*,3*S*)-3-(*tert*-butoxycarbonylamino)-2-hydroxy-4-phenylbutylamino)methyl)-2,2-dimethyloxazolidine-3-carboxylate 22. To a solution of the (*R*)-*tert*-butyl 4-(azidomethyl)-2,2-dimethyloxazolidine-3-carboxylate **21** (411 mg, 1.60 mmol) in MeOH (10 mL) was added Pd/C (40 mg). This mixture was stirred

at 23 °C under a hydrogen filled balloon for 2 h, then filtered over Celite, and the filter cake was washed with MeOH. Solvent was removed under reduced pressure, and the resultant residue was redisolved in *i*-PrOH, followed by addition of *tert*-butyl-[*S*-(*R*,*R*)]-(−)-(1-oxiranyl-2-phenylethyl)carbamate **7** (121 mg, 0.46 mmol). The mixture was allowed to stir at 65 °C for 24 h. Solvent was then removed under reduced pressure. Flash chromatography purification (2% MeOH in $CHCl_3$ as the eluent) yielded the (*R*)-amine **22** (93 mg, 41%) as a yellow oil. $R_f = 0.32$ (10% MeOH in $CHCl_3$); ^{1}H NMR (500 MHz, $CDCl_3$) δ 1.35 1(s, 18H), 1.48 (s, 24H), 1.54 (s, 3H), 1.58 (s, 3H), 2.67−2.92 (m, 10), 2.95 (d, 1H, $J = 4.1$ Hz), 2.98 (d, 1H, $J = 4.1$ Hz), 3.47 (brs, 2H), 3.78 (brs, 3H), 3.89−4.02 (m, 5H), 4.61 (brs, 1H), 4.68 (brs, 1H), 7.18−7.22 (m, 6H), 7.27−7.30 (m, 4H); ^{13}C NMR (125 MHz, $CDCl_3$) δ 22.9, 24.2, 26.6, 27.4, 28.1, 28.3, 36.4, 51.4, 56.9, 65.9, 70.7, 70.9, 79.3, 79.4, 79.6, 80.3, 93.4, 93.7, 126.2, 128.3, 129.4, 137.5, 137.7, 152.6, 155.8; LRMS-ESI (*m*/*z*) $[M + Na]^+$ 516.

(*R*)-*tert*-Butyl-4-((*N*-((2*R*,3*S*)-3-(*tert*-butoxycarbonylamino)-2-hydroxy-4-phenylbutyl)-4-methoxyphenylsulfonamido)methyl)-2,2-dimethyloxazolidine-3-carboxylate 23. To a stirred solution of amine **22** (37 mg, 0.07 mmol) in CH_2Cl_2 (4 mL) and aqueous saturated $NaHCO_3$ (4 mL) was added 4-methoxybenzenesulfonyl chloride (34 mg, 0.16 mmol). This reaction mixture was stirred for 12 h followed by extraction of the aqueous layer with CH_2Cl_2; the combined organic extracts were dried over anhydrous Na_2SO_4. Removal of solvent under reduced pressure followed by flash chromatography purification (30% EtOAc in hexane as the eluent) provided compound **23** (40 mg, 80%) as a white solid. $R_f = 0.37$ (40% EtOAc in hexane); ^{1}H NMR (500 MHz, $CDCl_3$) δ 1.34 (s, 9H), 1.48 (s, 9H), 1.60 (s, 6H), 2.84−2.89 (m, 1H), 2.95−3.06 (m, 2H), 3.15 (dd, 1H, $J = 6.5$, 13.0 Hz), 3.29 (d, 1H, $J = 9.7$ Hz), 3.41 (d, 1H, $J = 15.1$ Hz), 3.77 (brs, 2H), 3.85 (s, 3H), 3.90−3.94 (m, 1H), 3.99 (d, 1H, $J = 9.0$ Hz), 4.2 (brs, 1H), 4.73 (brs, 0.5H), 4.98 (brs, 0.5H), 6.95 (d, 2H, $J = 8.0$ Hz), 7.19−7.24 (m, 3H), 7.25−7.28 (m, 2H), 7.69 (d, 2H, $J = 8.9$ Hz); ^{13}C NMR (125 MHz, $CDCl_3$) δ 24.0, 27.4, 28.2, 28.3, 36.0, 53.3, 54.0, 55.4, 55.8, 56.3, 65.6, 72.4, 79.0, 80.9, 93.9, 114.2, 126.0, 128.1, 129.3, 129.6, 129.9, 137.8, 152.8, 155.4, 162.9; LRMS-ESI (*m*/*z*) $[M + Na]^+$ 686.

(*R*)-*tert*-Butyl-4-((*N*-((2*R*,3*S*)-3-(*tert*-butoxycarbonylamino)-2-hydroxy-4-phenylbutyl)-4-nitrophenylsulfonamido)methyl)-2,2-dimethyloxazolidine-3-carboxylate 24. To a stirred solution of amine **22** (41 mg, 0.08 mmol) in CH_2Cl_2 (4 mL) and aqueous saturated $NaHCO_3$ (4 mL) was added 4-nitrobenzenesulfonyl chloride (37 mg, 0.16 mmol). This reaction mixture was stirred for 12 h followed by extraction of the aqueous layer with CH_2Cl_2; the combined organic extracts were dried over anhydrous Na_2SO_4. Removal of solvent under reduced pressure followed by flash chromatography purification (30% EtOAc in hexane as the eluent) provided (*R*)-nitrosulfonamide **24** (51 mg, 92%) as a white solid. $R_f = 0.52$ (40% EtOAc in hexane); ^{1}H NMR (500 MHz, $CDCl_3$) δ 1.35 (s, 18H), 1.49 (s, 24H), 1.62 (s, 6H), 3.43 (bd, 2H, $J = 9.6$ Hz), 3.55 (d, 2H, $J = 15.1$ Hz), 3.75 (brs, 4H), 3.95 (s, 4H), 4.28 (brs, 2H), 4.63, (d, 2H, $J = 7.8$ Hz), 5.16 (brs, 2H), 7.19−7.23 (m, 6H), 7.25−7.31 (m, 4H), 7.92 (d, 4H, $J = 8.8$ Hz), 8.30 (d, 4H, $J = 8.05$ Hz); ^{13}C NMR (125 MHz, $CDCl_3$) δ 24.0, 27.3, 28.1, 28.2, 35.8, 53.7, 54.0, 55.5, 55.9, 65.6, 72.2, 79.4, 81.3, 94.1, 124.3, 126.3, 128.2, 128.4, 129.5, 137.4, 144.3, 149.9, 153.0, 155.5; LRMS-ESI (*m*/*z*) $[M + Na]^+$ 701.

***tert*-Butyl-(2*S*,3*R*)-3-hydroxy-4-(4-methoxy-*N*-(((*R*)-2-oxooxazolidin-4-yl)methyl)phenylsulfonamido)-1-phenylbutan-2-ylcarbamate 25.** To (*R*)-toluenesulfonate **23** (32 mg, 0.05 mmol) in methanol (3 mL) was added *p*-toluenesulfonic acid monohydrate (2 mg), and the reaction mixture was allowed to stir at 23 °C. After 12 h the reaction reached maximum conversion and did not move any further. It was quenched with saturated aqueous $NaHCO_3$, extracted with EtOAc, washed with water and brine, and dried over Na_2SO_4. Flash chromatography purification (30−50% EtOAc in hexane) yielded 7 mg (21%) of starting material and 18 mg (58%) of the expected primary alcohol.

The above alcohol (17 mg, 0.0278 mmol), in CH_2Cl_2 (2 mL) and Et_3N (16 μL, 0.11 mmol), was cooled to −10 °C and treated with methanesulfonyl chloride (2.5 μL, 0.03 mmol). The reaction mixture was stirred at 0 °C for 2 h, followed by removal of solvent via rotavap and pump. The resulting residue was redissolved in chloroform (2 mL), treated with DIPEA (19 μL, 0.11 mmol), refluxed for 8 h, and concentrated under reduced pressure. Flash chromatography purification (1% MeOH in $CHCl_3$ as the eluent) afforded (*R*)-oxazolidinone **25** (12 mg, 78%) as a white solid. $R_f = 0.33$ (5% MeOH in $CHCl_3$); ^{1}H NMR (500 MHz, $CDCl_3$) δ 1.32 (s, 9H), 2.77 (dd, 1H, $J = 8.4$, 13.9 Hz), 2.93−3.03 (m, 3H), 3.07 (d, 1H, $J = 14.5$ Hz), 3.13 (dd, 1H, $J = 9.3$, 14.1 Hz), 3.69−3.79 (m, 2H), 3.85 (s, 3H), 3.97 (dd, 1H, $J = 5.2$, 8.3 Hz), 4.23−4.29 (m, 1H), 4.43 (t, 1H, $J = 8.7$ Hz), 6.94 (d, 2H, $J = 8.8$ Hz), 7.18−7.24 (m, 3H), 7.26−7.30 (m, 2H), 7.64 (d, 2H, $J = 8.6$ Hz); ^{13}C NMR (125 MHz, $CDCl_3$) δ 28.1, 35.9, 52.0, 54.1, 54.6, 54.7, 55.5, 67.4, 71.9, 79.7, 114.4, 126.3, 128.4, 128.4, 129.3, 129.4, 137.5, 155.9, 159.4, 163.2; LRMS-ESI (*m*/*z*) $[M + Na]^+$ 572.

***tert*-Butyl-(2*S*,3*R*)-4-(4-amino-*N*-(((*R*)-2-oxooxazolidin-4-yl)-methyl)phenylsulfonamido)-3-hydroxy-1-phenylbutan-2-ylcarbamate 26.** To (*R*)-nitrosulfonamide **24** (42 mg, 0.06 mmol) in methanol (4 mL) was added *p*-toluenesulfonic acid monohydrate (2 mg), and the reaction mixture was allowed to stir at 23 °C. After 36 h the reaction appeared to have moved only 75% to completion, and formation of free amines was evident on TLC. At this point, it was quenched with saturated aqueous $NaHCO_3$, extracted with EtOAc, washed with water and brine, and dried over Na_2SO_4. Flash chromatography purification (30−50% EtOAc in hexane) yielded 7 mg (17%) of starting material and 24 mg (55%) of the expected primary alcohol.

The above alcohol (23 mg, 0.03 mmol), in CH_2Cl_2 (3 mL) and Et_3N (20 μL, 0.14 mmol), was cooled to −10 °C and treated with methanesulfonyl chloride (53 μL, 0.04 mmol). The reaction mixture was stirred at 0 °C for 2 h, followed by removal of solvent via rotavap and pump. The resultant residue was redissolved in chloroform (3 mL), treated with DIPEA (25 μL, 0.14 mmol), and refluxed for 12 h; product crashed out of the chloroform and was found to be only slightly soluble in methanol. Solvent was removed under reduced pressure, and the crude material was treated with methanol (3 mL) and Pd/C (3 mg). The mixture was stirred at 23 °C under a H_2 filled balloon for 2 h, then filtered over Celite, and the filter cake was washed with MeOH. Removal of solvent, followed by flash chromatography purification (3% MeOH in $CHCl_3$ as the eluent) provided (*R*)-oxazolidinone **26** (13 mg, 68%) as a white solid. $R_f = 0.19$ (5% MeOH in $CHCl_3$); ^{1}H NMR (500 MHz, $CDCl_3$) δ 1.31 (s, 9H), 2.73 (dd, 1H, $J = 8.7$, 13.6 Hz), 2.88 (dd, 1H, $J = 9.6$, 14.5 Hz), 2.91−2.94 (m, 1H), 2.98 (dd, 1H, $J = 4.2$, 13.9 Hz), 3.10 (dd, 2H, $J = 9.2$, 14.0 Hz), 3.70− 3.81 (m, 2H), 3.96 (dd, 1H, $J = 5.2$, 8.4 Hz), 4.21−4.24 (m, 1H), 4.40 (t, 1H, $J = 8.7$ Hz), 4.92 (d, 1H, $J = 8.5$ Hz), 6.63 (d, 2H, $J = 8.7$ Hz), 7.17−7.21 (m, 3H), 7.25−7.28 (m, 2H), 7.46 (d, 2H, $J = 8.4$ Hz); ^{13}C NMR (125 MHz, CD_3OD) δ 28.1, 29.5, 35.9, 51.9, 52.0, 54.0, 54.7, 67.5, 72.1, 79.6, 113.9, 124.4, 126.3, 128.3, 129.3, 129.4, 137.6, 155.1, 156.0, 159.5; LRMS-ESI (*m*/*z*) $[M + Na]^+$ 557.

tert*-Butyl-(2*S*,3*R*)-3-hydroxy-4-(4-methoxy-*N*-(((*S*)-2-oxooxazolidin-4-yl)methyl)phenylsulfonamido)-1-phenylbutan-2-ylcarbamate 27.** To a solution of the (*S*)-*tert*-butyl 4-(azidomethyl)-2,2-dimethyloxazolidine-3-carboxylate *ent*-**21** (840 mg, 3.32 mmol) in MeOH (20 mL) was added Pd/C (80 mg). This mixture was stirred at 23 °C under a hydrogen filled balloon for 2 h, then filtered over Celite, and the filter cake was washed with MeOH. Solvent was removed under reduced pressure, and the resultant residue was redissolved in *i*-PrOH, followed by addition of *tert*-butyl-[*S*-(*R*,*R*)]-(−)-(1-oxiranyl-2-phenylethyl)carbamate **7** (218 mg, 0.83 mmol). The mixture was allowed to stir at 65 °C for 24 h. Solvent was then removed under reduced pressure. Flash chromatography purification (2% MeOH in $CHCl_3$ as the eluent) yielded the corresponding (*S*)-amine (**22S*) (187 mg, 46%) as an amorphous solid. $R_f = 0.28$ (10% MeOH in $CHCl_3$); ^{1}H NMR (500 MHz, $CDCl_3$) δ 1.35 1(s, 18H), 1.48 (s, 24H), 1.54 (s, 3H), 1.58 (s, 3H), 2.64−2.91 (m, 10), 2.95−3.03 (m, 2H), 3.44 (brs, 1H), 3.50 (brs,

1H), 3.77 (brs, 3H), 3.87–4.00 (m, 5H), 4.61 (brs, 1H), 4.64 (brs, 1H), 7.18–7.22 (m, 6H), 7.27–7.30 (m, 4H); ^{13}C NMR (125 MHz, $CDCl_3$) δ 22.9, 24.2, 26.6, 27.4, 28.1, 28.3, 36.4, 51.4, 56.7, 56.8, 65.9, 70.6, 79.3, 79.6, 80.3, 93.4, 93.7, 126.2, 126.3, 128.3, 129.3, 137.6, 137.7, 152.5, 155.8; LRMS-ESI (*m/z*) $[M + Na]^+$ 576.

To a stirred solution of above *S*-amine (**22***S*) (85 mg, 0.17 mmol) in CH_2Cl_2 (6 mL) and aqueous saturated $NaHCO_3$ (6 mL) was added 4-methoxybenzenesulfonyl chloride (71 mg, 0.34 mmol). This reaction mixture was stirred for 12 h followed by extraction of the aqueous layer with CH_2Cl_2; the combined organic extracts were dried over anhydrous Na_2SO_4. Removal of solvent under reduced pressure followed by flash chromatography purification (30% EtOAc in hexane as the eluent) provided (*S*)-toluenesulfonate (**23***S*) (107 mg, 93%) as a white solid. $R_f = 0.40$ (40% EtOAc in hexane); ^{1}H NMR (500 MHz, $CDCl_3$) δ 1.34 (s, 18H), 1.46 (s, 24H), 1.58 (s, 6H), 2.82–2.87 (m, 2H), 2.96–3.13 (m, 4H), 3.18–3.24 (m, 3H), 3.32 (brs, 1H), 3.75 (brs, 1H), 3.80 (brs, 1H), 3.84 (s, 6H), 3.89–3.93 (4H), 4.07 (d, 2H, J = 9.2 Hz), 4.16–4.19 (m, 2H), 4.65 (brs, 1H), 4.87 (d, 1H, J = 7.31 Hz), 6.93–6.97 (m, 4H), 7.18–7.23 (6H), 7.26–7.28 (m, 4H), 7.64–7.71 (4H); ^{13}C NMR (125 MHz, $CDCl_3$) δ 23.9, 27.3, 28.1, 28.2, 35.6, 52.4, 54.3, 55.2, 55.4, 56.8, 65.6, 71.8, 79.1, 80.9, 93.8, 114.2, 126.1, 128.2, 129.3, 129.4, 129.6, 137.9, 152.6, 155.6, 162.8; LRMS-ESI (*m/z*) $[M + Na]^+$ 686.

To the above (*S*)-toluenesulfonate (**23***S*) (96 mg, 0.14 mmol) in methanol (5 mL) was added *p*-toluenesulfonic acid monohydrate (4.5 mg, 0.02 mmol), and the reaction mixture was allowed to stir at 23 °C. After 8 h the reaction reached maximum conversion and did not move any further. It was quenched with saturated aqueous $NaHCO_3$, extracted with EtOAc, washed with water and brine, and dried over Na_2SO_4. Flash chromatography purification (30–50% EtOAc in hexane) yielded 13 mg (13%) of starting material and 59 mg (65%) of the expected primary alcohol.

The above alcohol (58 mg, 0.09 mmol), in CH_2Cl_2 (4 mL) and Et_3N (33 μL, 0.23 mmol), was cooled to −10 °C and treated with methanesulfonyl chloride (7.9 μL, 0.1 mmol). The reaction mixture was stirred at 0 °C for 2 h, followed by removal of solvent via rotavap and pump. The resultant residue was redissolved in chloroform (4 mL), treated with DIPEA (65 μL, 0.37 mmol), refluxed for 12 h, and concentrated under reduced pressure. Flash chromatography purification (2% MeOH in $CHCl_3$ as the eluent) afforded *S*-oxazolidinone **27** (44 mg, 85%) as a white solid. R_f = 0.27 (5% MeOH in $CHCl_3$); ^{1}H NMR (500 MHz, CD_3OD) δ 1.27 (s, 9H), 2.52 (dd, 1H, J = 10.9, 13.7 Hz), 2.67 (dd, 1H, J = 8.9, 14.9 Hz), 2.83 (dd, 1H, J = 6.1, 14.0 Hz), 3.10 (dd, 1H, J = 3.5, 13.8 Hz), 3.47–3.52 (m, 2H), 3.58–3.63 (m, 1H), 3.80–3.83 (m, 1H), 3.85 (s, 3H), 4.23–4.29 (m, 1H), 4.31 (dd, 1H, J = 4.8, 8.9 Hz), 4.47 (t, 1H, J = 8.6 Hz), 7.06 (d, 2H, J = 8.93 Hz), 7.12–7.16 (m, 1H), 7.20–7.24 (m, 4H), 7.75 (d, 2H, J = 8.9 Hz); ^{13}C NMR (125 MHz, CD_3OD) δ 27.1, 35.6, 52.0, 54.3, 54.6, 54.7, 55.1, 68.0, 73.3, 78.5, 114.0, 125.5, 127.6, 128.9, 129.0, 129.3, 138.6, 156.5, 160.4, 163.3; LRMS-ESI (*m/z*) $[M + Na]^+$ 572.

tert*-Butyl-(2*S*,3*R*)-4-(4-amino-*N*-(((*S*)-2-oxooxazolidin-4-yl)-methyl)phenylsulfonamido)-3-hydroxy-1-phenylbutan-2-ylcarbamate 28.** To a stirred solution of *S*-amine (**22S*) (87 mg, 0.17 mmol) in CH_2Cl_2 (6 mL) and aqueous saturated $NaHCO_3$ (6 mL) was added 4-nitrobenzenesulfonyl chloride (78 mg, 0.35 mmol). This reaction mixture was stirred for 12 h followed by extraction of the aqueous layer with CH_2Cl_2; the combined organic extracts were dried over anhydrous Na_2SO_4. Removal of solvent under reduced pressure followed by flash chromatography purification (30% EtOAc in hexane as the eluent) provided *S*-nitrosulfonamide (**24***S*) (102 mg, 85%) as a yellow solid. R_f = 0.54 (40% EtOAc in hexane); ^{1}H NMR (500 MHz, $CDCl_3$) δ 1.34 (s, 18H), 1.47 (s, 24H), 1.59 (s, 6H), 2.81 (dd, 2H, J = 8.0, 12.9 Hz), 3.03 (bd, 2H, J = 9.7 Hz), 3.16–3.36 (m, 8H), 3.82 (brs, 2H), 3.91 (dd, 4H, J = 5.1, 8.7 Hz), 4.00 (d, 2H, J = 6.2 Hz), 4.20 (q, 2H, J = 5.6, 5.7 Hz), 4.80 (brs, 1H), 4.86 (d, 1H, J = 7.2 Hz), 7.20–7.24 (m, 6H), 7.27–7.30 (m, 4H), 7.88 (d, 4H, J = 8.4 Hz), 8.29 (d, 4H, J = 8.4 Hz); ^{13}C NMR (125 MHz, $CDCl_3$) δ 23.9, 27.3, 28.1, 28.2, 35.8, 52.3, 54.5, 54.9, 56.6, 65.5, 71.6, 79.5, 81.1, 94.0, 124.2, 126.3, 128.4, 128.4, 128.5, 129.3, 137.7, 144.0, 149.9, 152.7, 155.8, 171.0; LRMS-ESI (*m/z*) $[M + Na]^+$ 701.

To the above *S*-nitrosulfonamide (**24***S*) (92 mg, 0.13 mmol) in methanol (5 mL) was added *p*-toluenesulfonic acid monohydrate (4 mg, 0.02 mmol), and the reaction mixture was allowed to stir at 23 °C. After 18 h the reaction appeared to have moved only 50% to completion, and formation of free amines was evident on TLC. At this point it was quenched with saturated aqueous $NaHCO_3$, extracted with EtOAc, washed with water and brine, and dried over Na_2SO_4. Flash chromatography purification (30–50% EtOAc in hexane) yielded 32 mg (35%) of starting material and 44 mg (51%) of the expected primary alcohol.

The above alcohol (43 mg, 0.06 mmol), in CH_2Cl_2 (3 mL) and Et_3N (24 μL, 0.17 mmol), was cooled to −10 °C and treated with methanesulfonyl chloride (5.5 μL, 0.07 mmol). The reaction mixture was stirred at 0 °C for 2 h, followed by removal of solvent via rotavap and pump. The resultant residue was redissolved in chloroform (2 mL), treated with DIPEA (29 μL, 0.17 mmol), and refluxed for 12 h; product crashed out of the chloroform and was found to be only slightly soluble in methanol. Solvent was removed under reduced pressure, and the crude material was treated with methanol (4 mL) and Pd/C (5 mg). The mixture was stirred at 23 °C under a hydrogen filled balloon for 3 h, then filtered over Celite, and the filter cake was washed with MeOH. Removal of solvent followed by flash chromatography purification (3% MeOH in $CHCl_3$ as the eluent) provided (*S*)-oxazolidinone **28** (21 mg, 58%) as a white solid. R_f = 0.21 (5% MeOH in $CHCl_3$); ^{1}H NMR (500 MHz, 1:1 $CD_3OD/CDCl_3$) δ 1.24 (s, 9H), 2.54 (d, 1H), 2.56 (dd, 1H, J = 8.7, 14.9 Hz), 2.70 (dd, 1H, J = 7.6, 14.3 Hz), 2.97 (dd, 1H, J = 4.0, 13.9 Hz), 3.32 (dd, 1H, J = 5.0, 14.3 Hz), 3.38 (dd, 1H, J = 3.1, 14.8 Hz), 3.64–3.70 (m, 1H), 3.78–3.83 (m, 1H), 4.05 (dd, 1H, J = 5.3, 8.8 Hz), 4.16–4.20 (m, 1H), 4.39 (t, 1H, J = 8.7 Hz), 6.59 (d, 2H, J = 8.7 Hz), 7.09–7.15 (m, 3H), 7.18–7.21 (m, 2H), 7.40 (d, 2H, J = 8.7 Hz); ^{13}C NMR (125 MHz, 1:1 CD_3OD/$CDCl_3$) δ 31.8, 33.4, 39.4, 53.3, 56.9, 58.5, 58.8, 59.7, 71.8, 77.4, 83.3, 117.6, 127.4, 130.0, 132.0, 133.1, 133.2, 141.9, 156.0, 160.1, 164.0; LRMS-ESI (*m/z*) $[M + Na]^+$ 557.

(3*R*,3a*S*,6a*R*)-Hexahydrofuro[2,3-*b*]furan-3-yl-(2*S*,3*R*)-3-hydroxy-4-(4-methoxy-*N*-(((*R*)-2-oxooxazolidin-4-yl)methyl)phenylsulfonamido)-1-phenylbutan-2-ylcarbamate 29. A solution of *S*-aminosulfone **25** (10.9 mg, 0.02 mmol) in 30% trifluoroacetic acid (in CH_2Cl_2, 2 mL) was stirred at 23 °C for 40 min, then concentrated under reduced pressure. The residue was redissolved in CH_2Cl_2 (2 mL), treated with Et_3N (30 μL, 0.21 mmol), followed by carbonate **15** (6.3 mg, 0.02 mmol), and stirred at 23 °C for 12 h. The reaction mixture was then concentrated under reduced pressure and the residue was purified by flash chromatography (3% MeOH in $CHCl_3$ as the eluent) to give inhibitor **29** (10 mg, 85%) as a white solid. R_f = 0.54 (10% MeOH in $CHCl_3$); ^{1}H NMR (500 MHz, $CDCl_3$) δ 1.39 (dd, 1H, J = 5.5, 13.1 Hz), 1.56–1.63 (m, 1H), 2.67 (dd, 1H, J = 10.0, 14.0 Hz), 2.85–2.90 (m, 1H), 2.95–3.01 (m, 2H), 3.10 (dd, 1H, J = 4.1, 14.1 Hz), 3.20 (d, 1H, J = 12.8 Hz), 3.28 (dd, 1H, J = 9.2, 14.1 Hz), 3.63–3.72 (m, 1H), 3.73 (dd, 1H, J = 5.2, 9.8 Hz), 3.79 (dt, 1H, J = 1.6, 8.2 Hz), 3.86 (s, 3H), 3.88–3.95 (m, 3H), 4.04 (dd, 1H, J = 5.0, 8.8 Hz), 4.25 (brs, 1H), 4.28–4.34 (m, 1H), 4.47 (t, 1H, J = 8.7 Hz), 4.99 (q, 1H, J = 5.6, 13.4 Hz), 5.38 (d, 1H, J = 9.8 Hz), 5.63 (d, 1H, J = 5.2 Hz), 6.87 (s, 1H), 6.97 (d, 2H, J = 8.9 Hz), 7.16–7.22 (m, 3H), 7.24–7.28 (m, 2H), 7.69 (d, 2H, J = 8.8 Hz); ^{13}C NMR (125 MHz, $CDCl_3$) δ 25.8, 35.9, 45.4, 51.9, 54.1, 55.0, 55.3, 55.6, 67.6, 69.6, 71.1, 72.5, 73.4, 109.2, 114.5, 126.4, 128.4, 128.4, 129.2, 129.4, 137.5, 155.6, 159.6, 163.3; LRMS-ESI (*m/z*) $[M + Na]^+$ 628.2; HRMS-ESI (*m/z*) $[M + Na]^+$ calcd for $C_{28}H_{35}N_3O_{10}S$ 628.1941, found 628.1937.

(3*R*,3a*S*,6a*R*)-Hexahydrofuro[2,3-*b*]furan-3-yl-(2*S*,3*R*)-4-(4-amino-*N*-(((*R*)-2-oxooxazolidin-4-yl)methyl)phenylsulfonamido)-3-hydroxy-1-phenylbutan-2-ylcarbamate 30. A solution of the free amine **26** (12 mg, 0.02 mmol) in 30% trifluoroacetic acid in CH_2Cl_2 (2 mL) was stirred at 23 °C for 40 min, then concentrated under reduced pressure. The residue was redisolved in CH_2Cl_2 (2 mL), treated with carbonate **15** (7.1 mg, 0.02 mmol) and Et_3N (40

μL, 0.28 mmol), and stirred at 23 °C for 12 h at 40 °C. The reaction mixture was then concentrated under reduced pressure and the residue was purified by flash chromatography (5% MeOH in $CHCl_3$ as the eluent) to give inhibitor **30** (11 mg, 85%) as a white solid. $R_f = 0.26$ (10% MeOH in $CHCl_3$); ^{1}H NMR (500 MHz, $CDCl_3$) δ 1.38 (dd, 1H, $J = 5.6$, 13.2 Hz), 1.54−1.63 (m, 1H), 2.61 (dd, 1H, $J = 9.5$, 13.9 Hz), 2.83− 2.91 (m, 2H), 3.10 (d, 2H, $J = 13.3$ Hz), 3.18 (dd, 1H, $J = 9.6$, 13.9 Hz), 3.62−3.70 (m, 2H), 3.78−3.84 (m, 3H), 3.88 (dd, 1H, $J = 6.0$, 9.8 Hz), 3.97 (dd, 1H, $J = 5.0$, 8.9 Hz), 4.21−4.27 (m, 1H), 4.41 (t, 1H, $J = 8.7$ Hz), 4.93 (q, 1H, $J = 5.7$, 13.6 Hz), 5.60 (d, 1H, $J = 5.2$ Hz), 5.69 (d, 1H, $J = 8.8$ Hz), 6.64 (d, 2H, $J = 8.7$ Hz), 7.16−7.19 (m, 3H), 7.21−7.26 (m, 2H), 7.45 (d, 2H, $J = 8.7$ Hz); ^{13}C NMR (125 MHz, $CDCl_3$) δ 25.7, 29.5, 36.1, 45.3, 51.7, 54.1, 54.9, 55.1, 67.5, 69.5, 70.8, 71.0, 73.2, 109.2, 113.9, 123.9, 126.3, 128.3, 129.2, 129.4, 137.7, 151.4, 155.6, 159.6; LRMS-ESI (*m/z*) $[M + Na]^+$ 613.2; HRMS-ESI (*m/z*) $[M + Na]^+$ calcd for $C_{27}H_{34}N_4O_9S$ 613.1944, found 613.1939.

(3*R*,3a*S*,6a*R*)-Hexahydrofuro[2,3-*b*]furan-3-yl-(2*S*,3*R*)-3-hydroxy-4-(4-methoxy-*N*-(((*S*)-2-oxooxazolidin-4-yl)methyl)phenylsulfonamido)-1-phenylbutan-2-ylcarbamate 31. A solution of *S*-aminosulfonamide **27** (16.5 mg, 0.03 mmol) in 30% trifluoroacetic acid (in CH_2Cl_2, 3 mL) was stirred at 23 °C for 40 min, then concentrated under reduced pressure. The residue was redissolved in CH_2Cl_2 (3 mL), treated with Et_3N (41 μL, 0.29 mmol), followed by carbonate **15** (10 mg, 0.03 mmol), and stirred at 23 °C for 12 h. The reaction mixture was then concentrated under reduced pressure and the residue was purified by flash chromatography (3% MeOH in $CHCl_3$ as the eluent) to give inhibitor **31** (16 mg, 90%) as a white solid. $R_f = 0.5$ (10% MeOH in $CHCl_3$); ^{1}H NMR (500 MHz, $CDCl_3$) δ 1.32 (dd, 1H, $J = 5.4$, 13.2 Hz), 1.53−1.62 (m, 1H), 2.62 (dd, 1H, $J = 11.0$, 13.8 Hz), 2.71 (dd, 1H, $J = 7.25$, 14.6 Hz), 2.84−2.89 (m, 2H), 3.10 (dd, 1H, $J = 3.6$, 14.0 Hz), 3.61−3.67 (m, 1H), 3.74−3.82 (m, 2H), 3.86 (s, 3H), 3.87 (dd, 2H, $J = 5.8$, 10.1 Hz), 3.94−3.98 (m, 1H), 4.00−4.05 (m, 2H), 4.27−4.33 (m, 1H), 4.45 (t, 1H, $J = 8.8$ Hz), 4.99 (q, 1H, $J = 5.3$, 7.7 Hz), 5.60 (d, 1H, $J = 5.3$ Hz), 5.68 (d, 1H, $J = 9.2$ Hz), 6.98 (d, 2H, $J = 8.8$ Hz), 7.15−7.20 (m, 1H), 7.22−7.27 (m, 4H), 7.69 (d, 2H, $J = 8.8$ Hz); ^{13}C NMR (125 MHz, $CDCl_3$) δ 25.7, 43.4, 45.5, 53.2, 54.6, 54.9, 55.6, 56.5, 57.5, 69.6, 71.2, 73.3, 73.5, 109.3, 114.5, 126.3, 128.3, 129.2, 129.4, 137.8, 155.9, 159.61, 163.38; LRMS-ESI (*m/z*) $[M + Na]^+$ 628.2; HRMS-ESI (*m/z*) $[M + Na]^+$ calcd for $C_{28}H_{35}N_3O_{10}S$ 628.1941, found 628.1943.

(3*R*,3a*S*,6a*R*)-Hexahydrofuro[2,3-*b*]furan-3-yl-(2*S*,3*R*)-4-(4-amino-*N*-(((*S*)-2-oxooxazolidin-4-yl)methyl)phenylsulfonamido)-3-hydroxy-1-phenylbutan-2-ylcarbamate 32. A solution of the free amine **29** (15 mg, 0.03 mmol) in 30% trifluoroacetic acid (in CH_2Cl_2, 3 mL) was stirred at 23 °C for 40 min, then concentrated under reduced pressure. The residue was redissolved in CH_2Cl_2 (3 mL), charged with Et_3N (60 μL, 0.42 mmol), followed by carbonate **15** (8.9 mg, 0.03 mmol), and stirred at 23 °C for 12 h at 40 °C. The reaction mixture was then concentrated under reduced pressure and the residue was purified by flash chromatography (5% MeOH in $CHCl_3$ as the eluent) to give inhibitor **32** (13 mg, 80%) as a white solid. $R_f = 0.32$ (10% MeOH in $CHCl_3$); ^{1}H NMR (500 MHz, $CDCl_3$) δ 1.33 (dd, 1H, $J = 8.5$ Hz), 1.53−1.62 (m, 1H), 2.59 (dd, 1H, $J = 10.5$, 13.9 Hz), 2.66 (dd, 1H, $J = 7.4$, 14.7 Hz), 2.77 (dd, 1H, $J = 8.9$, 14.5 Hz), 2.82− 2.89 (m, 1H), 3.10 (dd, 1H, $J = 3.4$, 14.0 Hz), 3.36 (dd, 1H, $J = 3.5$, 14.3 Hz), 3.44 (dd, 1H, $J = 4.5$, 14.6 Hz), 3.62−3.67 (m, 1H), 3.72 (dd, 1H, $J = 5.0$, 9.9 Hz), 3.77 (dt, 1H, $J = 1.8$, 8.2 Hz), 3.87 (dd, 1H, $J = 5.8$, 9.9 Hz), 3.92−3.98 (m, 2H), 3.99 (dd, 1H, $J = 5.0$, 9.0 Hz), 4.15−4.29 (m, 1H), 4.43 (t, 1H, $J = 8.8$ Hz), 4.97 (q, 1H, $J = 5.4$, 13.2 Hz), 5.60 (d, 1H, $J = 5.3$ Hz), 6.66 (d, 2H, $J = 8.7$ Hz), 7.15−7.18 (m, 1H), 7.20−7.25 (m, 4H), 7.49 (d, 2H, $J = 8.6$ Hz); ^{13}C NMR (125 MHz, $CDCl_3$) δ 25.7, 29.5, 34.7, 45.5, 53.3, 54.6, 55.0, 56.6, 67.5, 69.6, 71.1, 73.4, 109.3, 114.0, 124.2, 126.3, 128.3, 129.2, 129.4, 137.8, 151.2, 155.8, 159.6; LRMS-ESI (*m/z*) $[M + Na]^+$ 613.2; HRMS-ESI (*m/z*) $[M + Na]^+$ calcd for $C_{27}H_{34}N_4O_9S$ 613.1944, found 613.1938.

Determination of X-ray Structure of 19b-Bound HIV Protease (WT). The stabilized HIV-1 protease with the substitutions of Q7K, L33I, L63I, C67A, and C95A that reduce autoproteolysis and aggregation[27] was expressed and purified as described.[28] These mutations do not alter the inhibitor binding site, and the stabilized protease has kinetic parameters and stability indistinguishable from those of the unsubstituted enzyme.[27,28] Inhibitor **19b** was dissolved in dimethyl sulfoxide (DMSO). Crystals were grown by the hanging drop vapor diffusion method using 1:5 molar ratio of protease (at 3.9 mg/mL) to inhibitor. The reservoir contained 0.1 M citrate phosphate buffer, pH 5.0, 0.35 M NaCl, and 4% DMSO. Crystals were mounted on a nylon loop and flash-frozen in liquid nitrogen with a cryoprotectant of 30% (v/v) glycerol. X-ray diffraction data were collected on the SER-CAT beamline of the Advanced Photon Source, Argonne National Laboratory. Diffraction data were processed using HKL2000 to 1.29 Å resolution.[28] Data were reduced in space group $P2_12_12$ with unit cell dimensions of $a = 58.11$ Å, $b = 86.42$ Å, $c = 45.97$ Å with one dimer in the asymmetric unit. The structure was solved by molecular replacement using the CCP4i,[29,30] using WT/GRL0255 complex (PDB 3DJK) as a starting model.[26] The structure was refined using SHELX97[31,32] and refitted manually using the molecular graphics program COOT.[33] Alternative conformations were modeled for the protease residues where observed in the electron density maps. Anisotropic atomic displacement parameters (*B*-factors) were refined for all atoms including solvent molecules. Hydrogen atoms were automatically added by SHELXL in the last round of the refinement. The identity of ions and other solvent molecules from the crystallization conditions was deduced from the shape and peak height of the $2F_o - F_c$ and $F_o - F_c$ electron density, the hydrogen bond interactions, and interatomic distances. The solvent molecules were one sodium ion, two chloride ions, one glycerol molecule, and 207 water (including partial occupancy sites). The final R was 14.1% for the working set, and R_{free} was 18.2% for all data between 10 and 1.29 Å resolution. The rmsd values from ideal bonds and angle distances were 0.013 and 0.031 Å, respectively. The average *B*-factor was 15.9 and 22.7 Å^2 for protease main chain and side chain atoms, respectively, 14.1 Å^2 for inhibitor atoms, and 32.1 Å^2 for water atoms. The crystallographic coordinates and structure factors have been deposited in the Protein Databank (PDB) with access code 3H5B.[34,35]

Acknowledgment. The research was supported by grants from the National Institutes of Health (Grant GM53386 to A.K.G. and Grant GM62920 to I.T.W.). This work was also supported by the Intramural Research Program of the Center for Cancer Research, National Cancer Institute, National Institutes of Health, and in part by a Grant-in-aid for Scientific Research (Priority Areas) from the Ministry of Education, Culture, Sports, Science, and Technology of Japan (Monbu Kagakusho), a Grant for Promotion of AIDS Research from the Ministry of Health, Welfare, and Labor of Japan (Kosei Rohdosho, Grant H15-AIDS-001), and the Grant to the Cooperative Research Project on Clinical and Epidemiological Studies of Emerging and Reemerging Infectious Diseases (Renkei Jigyo, No. 78, Kumamoto University) of Monbu-Kagakusho. We thank the staff at the SER-CAT beamline at the Advanced Photon Source, Argonne National Laboratory, for assistance during X-ray data collection. Use of the Advanced Photon Source was supported by the U.S. Department of Energy, Office of Science, Office of Basic Energy Sciences, under Contract No. DE-AC02-06CH11357.

Supporting Information Available: HPLC and HRMS data of inhibitors and crystallographic data. This material is available free of charge via the Internet at http://pubs.acs.org.

References

(1) (a) Flexner, C. HIV-protease inhibitors. *N. Engl. J. Med.* **1998**, *338*, 1281–1292. (b) Cihlar, T.; Bischofberger, N. Recent Developments

in Antiretroviral Therapies. In *Annual Reports in Medicinal Chemistry*; Academic Press: San Diego, CA, 2000; Vol. 35, Chapter 16, pp 177–189.
(2) Sepkowitz, K. A. AIDS, the first 20 years. *N. Engl. J. Med* **2001**, *344*, 1764–1772.
(3) UNAIDS/WHO Report on Annual AIDS Epidemic Update; United Nations Publications, December 2008. http://www.unaids.org/epi/2008/.
(4) (a) Waters, L.; Nelson, M. Why do patients fail HIV therapy? *Int. J. Clin. Pract.* **2007**, *61*, 983–990. (b) Grabar, S.; Pradier, C.; Le Corfec, E.; Lancar, R.; Allavena, C.; Bentata, M.; Berlureau, P.; Dupont, C.; Fabbro-Peray, P.; Poizot-Martin, I.; Costagliola, D. Factors associated with clinical and virological failure in patients receiving a triple therapy including a protease inhibitor. *AIDS* **2000**, *14*, 141–149.
(5) (a) Pillay, D.; Bhaskaran, K.; Jurriaans, S.; Prins, M.; Masquelier, B.; Dabis, F.; Gifford, R.; Nielsen, C.; Pedersen, C.; Balotta, C.; Rezza, G.; Ortiz, M.; de Mendoza, C.; Kucherer, C.; Poggensee, G.; Gill, J.; Porter, K. The impact of transmitted drug resistance on the natural history of HIV infection and response to first-line therapy. *AIDS* **2006**, *20*, 21–28. (b) Wainberg, M. A.; Friedland, G. Public health implications of antiretroviral therapy and HIV drug resistance. *JAMA, J. Am. Med. Assoc.* **1998**, *279*, 1977–1983.
(6) Yerly, S.; Kaiser, L.; Race, E.; Bru, J. P.; Clavel, F.; Perrin, L. Transmission of antiretroviral drug resistant HIV-1 variants. *Lancet* **1999**, *354*, 729–733.
(7) (a) Ghosh, A. K.; Kincaid, J. F.; Cho, W.; Walters, D. E.; Krishnan, K.; Hussain, K. A.; Koo, Y.; Cho, H.; Rudall, C.; Holland, L.; Buthod, J. Potent HIV protease inhibitors incorporating high-affinity P2-ligands and (*R*)-(hydroxyethylamino)sulfonamide isostere. *Bioorg. Med. Chem. Lett.* **1998**, *8*, 687–690. (b) Ghosh, A. K.; Shin, D.; Swanson, L.; Krishnan, K.; Cho, H.; Hussain, K. A.; Walters, D. E.; Holland, L.; Buthod, J. Structure-based design of non-peptide HIV protease inhibitors. *Farmaco* **2001**, *56*, 29–32. (c) Ghosh, A. K.; Sridhar, P. R.; Kumaragurubaran, N.; Koh, Y.; Weber, I. T.; Mitsuya, H. Bis-tetrahydrofuran: a privileged ligand for darunavir and a new generation of HIV protease inhibitors that combat drug resistance. *ChemMedChem* **2006**, *1*, 939–950.
(8) (a) Yoshimura, K.; Kato, R.; Kavlick, M. F.; Nguyen, A.; Maroun, V.; Maeda, K.; Hussain, K. A.; Ghosh, A. K.; Gulnik, S. V.; Erickson, J. W.; Mitsuya, H. A potent human immunodeficiency virus type 1 protease inhibitor, UIC-94003 (TMC-126), and selection of a novel (A28S) mutation in the protease active site. *J. Virol.* **2002**, *76*, 1349–1358. (b) Koh, Y.; Nakata, H.; Maeda, K.; Ogata, H.; Bilcer, G.; Devasamudram, T.; Kincaid, J. F.; Boross, P.; Wang, Y. F.; Tie, Y.; Volarath, P.; Gaddis, L.; Harrison, R. W.; Weber, I. T.; Ghosh, A. K.; Mitsuya, H. Novel bis-tetrahydrofuranylurethane-containing nonpeptidic protease inhibitor (PI) UIC-94017 (TMC114) with potent activity against multi-PI-resistant human immunodeficiency virus in vitro. *Antimicrob. Agents Chemother.* **2003**, *47*, 3123–3129.
(9) Ghosh, A. K.; Sridhar, P. R.; Leshchenko, S.; Hussain, A. K.; Li, J.; Kovalevsky, A.; Walters, D. E.; Wedekind, J. E.; Grum-Tokars, V.; Das, D.; Koh, Y.; Maeda, K.; Gatanaga, H.; Weber, I. T.; Mitsuya, H. Structure-based design of novel HIV-1 protease inhibitors to combat drug resistance. *J. Med. Chem.* **2006**, *49*, 5252–5261.
(10) FDA approved darunavir on June 23, 2006. FDA approved new HIV treatment for patients who do not respond to existing drugs. Please see the following site: http://www.fda.gov/bbrs/topics/NEWS/2006/NEW01395.htmL.
(11) On October 21, 2008, FDA granted traditional approval to Prezista (darunavir), coadministered with ritonavir and with other antiretroviral agents, for the treatment of HIV-1 infection in treatment-experienced adult patients. In addition to the traditional approval, a new dosing regimen for treatment-naive patients was approved.
(12) Ghosh, A. K.; Chapsal, B. D.; Weber, I. T.; Mitsuya, H. Design of HIV protease inhibitors targeting protein backbone: an effective strategy for combating drug resistance. *Acc. Chem. Res.* **2008**, *41*, 78–86.
(13) Hong, L.; Zhang, X. C.; Hartsuck, J. A.; Tang, J. Crystal structure of an in vivo HIV-1 protease mutant in complex with saquinavir: insights into the mechanisms of drug resistance. *Protein Sci.* **2000**, *9*, 1898–1904.
(14) (a) Tie, Y.; Kovalevsky, A. Y.; Boross, P.; Wang, Y. F.; Ghosh, A. K.; Tozser, J.; Harrison, R. W.; Weber, I. T. Atomic resolution crystal structures of HIV-1 protease and mutants V82A and I84V with saquinavir. *Proteins* **2007**, *67*, 232–242. (b) Kovalevsky, A. Y.; Tie, Y.; Liu, F.; Boross, P. I.; Wang, Y. F.; Leshchenko, S.; Ghosh, A. K.; Harrison, R. W.; Weber, I. T. Effectiveness of nonpeptide clinical inhibitor TMC-114 on HIV-1 protease with highly drug resistant mutations D30N, I50V, and L90M. *J. Med. Chem.* **2006**, *49*, 1379–1387.
(15) (a) Tie, Y.; Boross, P. I.; Wang, Y. F.; Gaddis, L.; Hussain, A. K.; Leshchenko, S.; Ghosh, A. K.; Louis, J. M.; Harrison, R. W.; Weber, I. T. High resolution crystal structures of HIV-1 protease with a potent non-peptide inhibitor (UIC-94017) active against multi-drug-resistant clinical strains. *J. Mol. Biol.* **2004**, *338*, 341–352. (b) Amano, M.; Koh, Y.; Das, D.; Li, J.; Leschenko, S.; Wang, Y. F.; Boross, P. I.; Weber, I. T.; Ghosh, A. K.; Mitsuya, H. A novel bis-tetrahydrofuranylurethane-containing nonpeptidic protease inhibitor (PI), GRL-98065, is potent against multiple-PI-resistant human immunodeficiency virus in vitro. *Antimicrob. Agents Chemother.* **2007**, *51*, 2143–2155.
(16) (a) Ghosh, A. K.; Leshchenko, S.; Noetzel, M. Stereoselective photochemical 1,3-dioxalene addition to 5-alkoxymethyl-2(5*H*)-furanone: synthesis of bis-tetrahydrofuranyl ligand for HIV protease inhibitor UIC-94017 (TMC-114). *J. Org. Chem.* **2004**, *69*, 7822–7829. (b) Ghosh, A. K.; Li, J.; Ramu, S. P. A stereoselective anti-aldol route to (3*R*,3a*S*,6a*R*)-tetrahydro-2*H*-furo[2,3-*b*]furan-3-ol: a key ligand for a new generation of HIV protease inhibitors. *Synthesis* **2006**, 3015–3019.
(17) (a) Ghosh, A. K.; Duong, T. T.; McKee, S. P. Di(2-pyridyl) carbonate promoted alkoxycarbonylation of amines: a convenient synthesis of functionalized carbamates. *Tetrahedron Lett.* **1991**, *32*, 4251–4254. (b) Ghosh, A. K.; Duong, T. T.; McKee, S. P.; Thompson, W. J. *N,N'*-Dissuccinimidyl carbonate: a useful reagent for alkoxycarbonylation of amines. *Tetrahedron Lett.* **1992**, *33*, 2781–2784.
(18) (a) Dondoni, A.; Perrone, D. Synthesis of 1,1-Dimethylethyl (*S*)-4-Formyl-2,2-dimethyl-3-oxazolidinecarboxylate by Oxidation of the Alcohol. *Organic Syntheses*; Wiley & Sons: New York, 2004; Collect. Vol. 10, p 320. Dondoni, A.; Perrone, D. *Org. Synth.* **2000**, *77*, 64. (b) Dondoni, A.; Giovannini, P. P.; Massi, A. Assembling heterocycle-tethered C-glycosyl and α-amino acid residues via 1,3-dipolar cycloaddition reactions. *Org. Lett.* **2004**, *6*, 2929–2932.
(19) Toth, M. V.; Marshall, G. R. A simple, continuous fluorometric assay for HIV protease. *Int. J. Pept. Protein Res.* **1990**, *36*, 544–550.
(20) Koh, Y.; Das, D.; Leshchenko, S.; Nakata, H.; Ogata-Aoki, H.; Amano, M.; Nakayama, M.; Ghosh, A. K.; Mitsuya, H. GRL-0 2031 a novel nonpeptide protease inhibitor (PI) containing a stereochemistry defined fused cyclopentanyltetrahydrofuran (Cp-THF) potent against multi-PI-resistant HIV-1 in vitro. *Antimicrob. Agents Chemother.*, in press.
(21) Gustchina, A.; Sansom, C.; Prevost, M.; Richelle, J.; Wodak, S.; Wlodawer, A.; Weber, I. Energy calculations and analysis of HIV-1 protease-inhibitor crystal structures. *Protein Eng.* **1994**, *7*, 309–317.
(22) Tie, Y.; Boross, P. I.; Wang, Y. F.; Gaddis, L.; Liu, F.; Chen, X.; Tozser, J.; Harrison, R. W.; Weber, I. T. Molecular basis for subrstrate recognition and drug resistance from 1.1 to 1.6 Å resolution crystal structures of HIV-1 protease mutants with subrstrate analogs. *FEBS J.* **2005**, *272*, 5265–5277.
(23) Panigrahi, S.; Desiraju, G. Strong and weak hydrogen bonds in the protein–ligand interface. *Proteins* **2007**, *67*, 128–141.
(24) Steiner, T. Hydrogen bonds from water molecules to aromatic acceptors in very high-resolution protein crystal structures. *Biophys. Chem.* **2002**, *95*, 195–201.
(25) Wang, Y. F.; Tie, Y.; Boross, P. I.; Tozser, J.; Ghosh, A. K.; Harrison, R. W.; Weber, I. T. Potent new antiviral compound shows similar inhibition and structural interactions with drug resistant mutants and wild type HIV-1 protease. *J. Med. Chem.* **2007**, *50*, 4509–4515.
(26) Ghosh, A. K.; Gemma, S.; Baldridge, A.; Wang, Y. F.; Kovalevsky, A. Y.; Koh, Y.; Weber, I. T.; Mitsuya, H. Flexible cyclic ethers/polyethers as novel P2-ligands for HIV-1 protease inhibitors: design, synthesis, biological evaluation, and protein–ligand X-ray studies. *J. Med. Chem.* **2008**, *51*, 6021–6033.
(27) Louis, J. M.; Clore, G. M.; Gronenborn, A. M. Autoprocessing of HIV-1 protease is tightly coupled to protein folding. *Nat. Struct. Biol.* **1999**, *6*, 868–875.
(28) Mahalingam, B.; Louis, J. M.; Hung, J.; Harrison, R. W.; Weber, I. T. Structural implications of drug resistant mutants of HIV-1 protease: high resolution crystal structures of the mutant protease/subrstrate analog complexes. *Proteins* **2001**, *43*, 455–464.
(29) Otwinowski, Z.; Minor, W. Processing of X-ray diffraction data in oscillation mode. *Methods Enzymol.* **1997**, *276*, 307–326.
(30) Collaborative Computational Project, number 4. The CCP4 suite: programs for protein crystallography. *Acta Crystallogr.* **1994**, *D50*, 760–763.
(31) Potterton, E.; Briggs, P.; Turkenburg, M.; Dodson, E. A graphical user interface to the CCP4 program suite. *Acta Crystallogr.* **2003**, *D59*, 1131–1137.
(32) Sheldrick, G. M.; Schneider, T. R. SHELXL: high resolution refinement. *Methods Enzymol.* **1997**, *277*, 319–343.
(33) Jones, T. A.; Zou, J. Y.; Cowan, S. W.; Kjeldgaard, M. Improved methods for building protein models in electron density maps and the location of errors in these models. *Acta Crystallogr.* **1991**, *A47*, 110–119.
(34) Emsley, P.; Cowtan, K. Coot: model-building tools for molecular graphics. *Acta Crystallogr.* **2004**, *D60*, 2126–2132.
(35) Berman, H. M.; Westbrook, J.; Feng, Z.; Gilliland, G.; Bhat, T. N.; Weissig, H.; Shindyalov, I. N.; Bourne, P. E. The Protein Data Bank. *Nucleic Acids Res.* **2000**, *28*, 235–242.

JM900303M

P-Glycoprotein Mediates Efflux Transport of Darunavir in Human Intestinal Caco-2 and ABCB1 Gene-Transfected Renal LLC-PK1 Cell Lines

Hiromi FUJIMOTO,[a,#] Maiko HIGUCHI,[a,#] Hiroshi WATANABE,[a] Yasuhiro KOH,[b] Arun K. GHOSH,[c] Hiroaki MITSUYA,[b] Naomi TANOUE,[a] Akinobu HAMADA,[a] and Hideyuki SAITO*[,a]

[a] *Department of Pharmacy, Kumamoto University Hospital;* [b] *Department of Hematology, Kumamoto University Graduate School of Medical and Pharmaceutical Sciences, Kumamoto University; 1–1–1 Honjo, Kumamoto 860–8556, Japan:* [c] *Departments of Chemistry and Medicinal Chemistry, Purdue University; West Lafayette, Indiana 47907, U.S.A.*

Received April 2, 2009; accepted July 4, 2009; published online July 6, 2009

Darunavir (DRV) is a nonpeptidic protease inhibitor (PI) approved for the treatment of human immunodeficiency virus (HIV) infection. DRV displays potent activity against HIV strains resistant to other available PIs. Coadministration with ritonavir (RTV) improves the oral bioavailability of DRV. Inhibition of cytochrome P450 by RTV has been proposed as a mechanism for enhanced DRV bioavailability. However, interaction of these drugs with intestinal transporters has not been elucidated. This study was performed to explore the involvement of P-glycoprotein in transcellular DRV transport in monolayers of human intestinal Caco-2 and in ABCB1 multidrug resistance 1, (MDR1) gene-transfected renal LLC-PK1 (L-MDR1) cell lines. Transepithelial transport of DRV in Caco-2 cell monolayers was 2-fold greater in the basal-to-apical direction compared to that in the opposite direction. RTV had a significant inhibitory effect on the efflux transport of DRV in Caco-2 cells. The apical-to-basal DRV transport was enhanced by P-glycoprotein inhibitors, cyclosporin A and verapamil, as well as multidrug resistance-related protein (MRP/ABCC) inhibitors, probenecid and MK571. Using the L-MDR1 cell line, basal-to-apical DRV transport was much greater than in the opposite direction. Furthermore, cyclosporin A markedly inhibited the basal-to-apical DRV transport. RTV significantly increased the apical-to-basal transport of DRV in L-MDR1 cells, but reduced transport in the opposite direction. DRV inhibited P-glycoprotein-mediated efflux of calcein-acetoxymethyl ester in L-MDR1 cells with the inhibitory potency of 121 μM. These findings suggest that DRV is a substrate of P-glycoprotein and MRP, most likely MRP2. RTV appeared to inhibit P-glycoprotein, thereby enhancing the absorptive transport of DRV.

Key words protease inhibitor; transcellular transport; P-glycoprotein; Caco-2 cell

Treatment regimens for human immunodeficiency virus (HIV) infection have been greatly improved by the development of novel classes of anti-HIV drugs, including nucleoside analogues (NRTI), non-nucleoside analogue reverse transcriptase inhibitors (NNRTI) and protease inhibitors (PI). The term highly active antiretroviral therapy (HAART) is used to describe a combination of three or more of these anti-HIV drugs.[1,2] During HAART, plasma HIV-1 levels rapidly decline to below the detection limit of standard clinical assays. However, reactivation of the remaining latently infected memory $CD4^+$-T cells appears to be a source of continued virus reproduction.[3] Virologic response to HAART treatment depends on viral sensitivity to antiretroviral drugs as well as patient compliance and medication adherence.[1] However, long-term HAART treatment has raised issues concerning the development of drug-resistant HIV-1 variants[4,5] and chronic side effects caused by the drugs.[6,7] With the initiation of HAART, patients generally receive a combination of two NRTIs and either NNRTI or PI. The Department of Health and Human Services recommends an initial treatment regimen with the combination of tenofovir/emtricitabine or zidovudine/lamivudine as the NRTIs and either efavirenz as an NNRTI or atazanavir with ritonavir, fosamprenavir with ritonavir (RTV), or lopinavir/RTV as the PIs.[8] However, virological failure continues to occur in a substantial proportion of HIV-infected patients who have received HAART.[9]

Darunavir (DRV), formerly TMC-114, is a novel approved PI for the treatment of HIV infection.[10,11] It was originally designed to be active against HIV strains resistant to other currently available PIs.[12] POWER trials have evaluated the safety and efficacy of DRV in treatment-experienced HIV patients previously given other PIs.[13] In these studies, DRV has indicated a significantly greater reduction in plasma HIV-RNA and an increase in CD4 counts compared with the active controls for patients with extensive PI resistance. Currently, there is a paucity of information on DRV resistance. Indeed, such data is mainly derived from clinical trials conducted during the registration of DRV. It is known that DRV is rapidly absorbed from the intestine after oral administration, reaching peak plasma concentrations after 2.5—4.0 h.[14] Absorption of DRV is followed by a fast distribution/elimination phase and a subsequent slower elimination phase with a terminal elimination half-life of 15 h in the presence of low-dose RTV as a boosting drug.[14,15] DRV is extensively metabolized by intestinal and hepatic cytochrome P450 (CYP) 3A4. Coadministration with small doses of RTV (100 mg) is thought to inhibit hepatic CYP3A4 activity, resulting in an increase in oral DRV bioavailability from 37 to 82%. DRV and its metabolites are mainly excreted in feces (80%), and, to a lesser extent, in urine (14%).[15] Most PIs are reported to suppress intestinal ABCB1/P-glycoprotein mediated drug efflux into the lumen.[16,17] However, there are no reports whether DRV *per se* is a transport substrate of P-glycoprotein.

The purpose of this study was to investigate the involvement of P-glycoprotein in transcellular transport of DRV across monolayers of the human intestinal epithelial Caco-2 cell line and the renal epithelial LLC-PK1 cell line stably

* To whom correspondence should be addressed. e-mail: saitohide@fc.kuh.kumamoto-u.ac.jp
# These authors contributed equally to this work.

transfected with the ABCB1 gene.

MATERIALS AND METHODS

Chemicals Saquinavir (SQV) was obtained form Nippon Roche Co. (Tokyo Japan). Nelfinavir (NFV) and ritonavir (RTV) were a gift from JT Co. (Tokyo Japan) and Abbott Laboratories Co. (Illinois, U.S.A.), respectively. Darunavir (DRV) was synthesized in a convergent manner as previously described by Ghosh *et al.*[10] Cylcosporin A was obtained from Novartis Pharma (Basel, Switzerland). Verapamil, probenecid, novobiocin, rifamycin SV, bromosulfophthalien, glycylleucine and glyclylsarcosine were purchased from Sigma-Aldrich (St. Louis, MO, U.S.A.). MK571 was obtained from BIOMOL International, L.P. (Plymouth Meeting, PA, U.S.A.). Calcein-acetoxymethyl (AM) ester was purchased from Molecular Probe Co. (Eugene, OR, U.S.A.). All other chemicals used were of the highest purity available.

Cell Cultures Caco-2 cells at passage 18, obtained from the American Type Culture Collection (ATCC HTB37), were maintained by serial passage in plastic culture dishes as described previously.[18] For the transport studies, Caco-2 cells were seeded on polycarbonate membrane filters (3-μm pores, 4.71-cm^2 growth area) inside Transwell cell culture chambers (Costar; Cambridge, MA, U.S.A.) at a cell density of 3×10^5 cells/well. The Transwell chambers were placed in six-well tissue culture plates with 2.6 ml of medium outside (basal chamber) and 1.5 ml of medium inside (apical chamber). The medium consisted of Dulbecco's modified Eagle's medium (Sigma-Aldrich) supplemented with 10% fetal bovine serum (BioReliance; Rockville, MD, U.S.A.) and 1% nonessential amino acids (Invitrogen; Carlsbad, CA, U.S.A.) without antibiotics. The cells were grown in an atmosphere of 5% CO_2, 95% air at 37 °C, and given fresh medium every 2 or 3 d. Cells were cultured for a total of 14 d. In this study, cells between the 37th and 50th passage were used. Porcine kidney epithelial LLC-PK1 and L-MDR1 cells transfected with human ABCB1 cDNA (generous gifts from Dr. Erin G. Schuetz, St. Jude Children's Research Hospital, Memphis, TN, U.S.A.) were cultured as described previously.[19] In brief, LLC-PK1 and L-MDR1 cells were maintained in complete medium consisting of Medium 199 supplemented with 10% fetal bovine serum and 1% penicillin and streptomycin, and L-MDR1 cells were maintained at 640 nM vincristine. For the transport studies, L-MDR1 and LLC-PK1 cells were seeded on polycarbonate membrane filters (3.0-μm pores, 4.71-cm^2 growth area) inside Transwell cell culture chambers at a cell density of 2×10^6 cells/filter. Cells in each chamber were cultured as described above for 3 d. The medium was replaced by fresh medium after 2 d, and the cells were used in the transport studies 3 d after inoculation.

Transcellular Transport and Intracellular Accumulation of DRV Transcellular transport of DRV was determined using cell monolayers grown in Transwell chambers. Culture medium on either the basal or apical side of the monolayers was replaced with 2 ml of incubation medium [145 mM NaCl, 3 mM KCl, 1 mM $CaCl_2$, 0.5 mM $MgCl_2$, 5 mM D-glucose, 8 mM Na_2HPO_4, 1.5 K_2HPO_4 and 5 mM *N*-(2-hydroxyethyl)piperazine-*N'*-2-ethanesulfonic acid (HEPES) (pH 7.4) or MES (pH 6.0)] containing DRV (10 μM) with or without PI, and medium on the opposite side was replaced with 2 ml of fresh incubation medium. In inhibition study, an inhibitor was added to the incubation medium on both sides of the monolayer. The monolayers were incubated in 5% CO_2–95% air at 37 °C for up to 6 h, and 130 μl aliquots of medium from the relevant side were taken at the indicated time points. For accumulation studies, the medium was aspirated off at the end of the incubation period, and the monolayers were washed twice with 2 ml of ice-cold incubation medium. The filters with cell monolayers were immersed in 1 ml of extraction solution composed of the mobile phase of HPLC assay/methanol (1 : 1) for 1 h. Supernatants obtained after centrifugation at 200 ***g*** for 15 min were used for the HPLC assay. The remaining cells were lysed with 1 ml of 1 N NaOH, and used for the protein assay using a Bio-Rad protein assay kit (Bio-Rad Laboratories; Richmond, CA, U.S.A.) with bovine γ-globulin as a standard.

Calcein-AM Efflux Assay Efflux assays were performed as described previously.[19] A kinetic fluorometric assay was used to study the interaction of DRV with P-glycoprotein. For the calcein-AM efflux assay, L-MDR1 and LLC-PK1 cells were seeded in 96-well tissue culture plates at a cell density of 1×10^5 cells/well. Cells were cultured in 200 μl of Medium 199 supplemented with 10% fetal bovine serum in each well in an atmosphere of 5% CO_2–95% air at 37 °C for 1 d. Cells were plated in 96-well tissue culture plates in Medium 199 containing PI. After a 30-min incubation period, calcein-AM was added to a final concentration of 2 μM, and the plates were placed into a Fluoroscan Ascent Thermo Labsystems, Franklin, MA, U.S.A.). Fluorescence was measured from 0 to 30 min using an excitation of 485 nm and an emission of 530 nm. The rate of calcein accumulation in the presence and absence of DRV was calculated by linear regression analysis using the Ascent software (Thermo Labsystems). Inhibitory potency of DRV for P-glycoprotein was evaluated by fluorescence at 30 min as a percentage of LLCmax, ((L-MDR1[I])−(L-MDR1[0]))×100/((LLC-PK1[0])−(L-MDR1[0])), where [I] represents a concentration of DRV, and [0] means absence of DRV.[20]

HPLC Detrermination of DRV The concentration of DRV was determined using HPLC (model LC-6A; Shimadzu, Kyoto, Japan). One hundred ml of sample were injected into the HPLC column. Separation was performed on a reversed-phase column (Zorbax SB-C18, 5-μm particle size, 150 mm×4 mm i.d.) at 40 °C. The mobile phase was a mixture of solution containing 25 mM sodium acetate and 25 mM hexane-1-sulfuric acid (pH 6.0) and acetonitrile (57 : 43). The flow rate was 1.0 ml/min and DRV was detected by UV absorption at 268 nm. The recovery of known small amount of DRV applied on cell monolayers for 60 min in the extraction method was >93%.

Statistical Analysis Data were analyzed statistically by analysis of variance (ANOVA) followed by Scheffe's multiple comparison test. A p-value of less than 0.05 was considered statistically significant.

RESULTS

Effect of RTV on the Transepithelial Transport of DRV in Caco-2 Cell Monolayers Transepithelial transport of DRV (10 μM) in the apical-to-basal direction was time-dependent. Approximately 20% of the applied DRV in the api-

cal chamber permeated into the basal compartment after 6 h (Fig. 1). The basal-to-apical transport of DRV was also time-dependent, with 43% of the applied DRV dose found in the opposite compartment after 6 h. These findings suggest that transepithelial transport of DRV is two-fold greater in the basal-to-apical direction compared to the opposite direction, corresponding to intestinal secretory transport. The apical-to-basal transport of DRV in the presence of RTV (20 μM) was significantly elevated compared to that in the absence of RTV. In contrast, the basal-to-apical transport of DRV was unaffected by the presence of RTV. The results indicate that the presence of RTV in the apical compartment had an inhibitory effect on efflux transport of DRV in the apical membranes of Caco-2 cells. The apical-to-basal transport of DRV in the presence of either cyclosporin A or verapamil, representative inhibitors of P-glycoprotein, was significantly increased compared to that in the absence of inhibitors (data not shown).

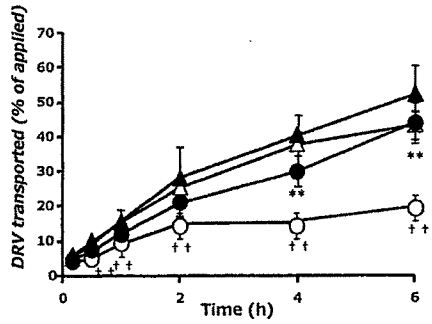

Fig. 1. Effect of RTV on the Transepithelial Transport of DRV in Monolayers of Caco-2 Cells

Transport of DRV (10 μM) in the apical-to-basal direction (○, ●) and in the basal-to-apical direction (△, ▲) in the absence (control, open symbol) or presence (closed symbol) of RTV (20 μM). Each point represents the mean±S.D. of three independent measurements. $^{**}p<0.01$, significantly different from apical-to-basal transport without RTV. $^{\dagger\dagger}p<0.01$, significantly different from basal-to-apical transport without RTV.

Effects of Various Inhibitors on Transcellular Transport of DRV in Caco-2 Cell Monolayers The apical-to-basal transport of DRV was significantly increased in the presence of cyclosporin A, verapamil, probenecid, MK571, rifamycin SV and bromosulfophthalein (BSP) (Fig. 2). Probenecid and MK571 have been reported to inhibit multidrug resistant-associated protein (MRP/ABCC) 2.[22] Rifamycin SV and BSP are known to inhibit organic anion transporting protein (OATP/SLCO) family members OATP1B1 and OATP1B3, respectively.[23] In contrast, novobiocin, an inhibitor for breast cancer resistance protein (BCRP/ABCG2),[24] significantly enhances the basal-to-apical transport of DRV. Glycylleucine and glycylsarcosine, a substrate and inhibitor of H^+/oligopeptide cotransporter PEPT1 (SLC15A1), respectively,[18] had no effect on the DRV transport. The ratio of basal-to-apical transport to apical-to-basal transport indicates that cyclosporin A, verapamil and RTV strongly suppressed the net secretory transepithelial transport of DRV. Probenecid, MK571 rifamycin SV and BSP had weak but significant inhibitory effects on the secretory transport of DRV. However, novobiocin markedly stimulated the secretory transport of DRV.

Effect of Cyclosporin A and Verapamil on Transepithe-

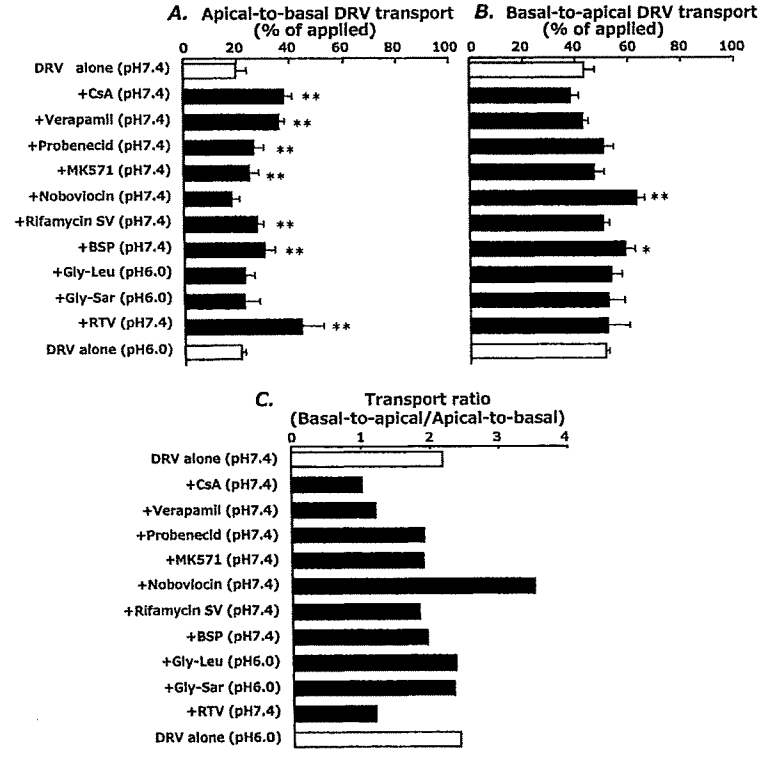

Fig. 2. Effect of Various Inhibitors on Transepithelial Transport of DRV in Monolayers of Caco-2 Cells 6 h after Incubation with DRV

Apical-to-basal transport (A), basal-to-apical transport (B) and the transport ratio of basal-to-apical transport divided by apical-to-basal transport (C). Each bar represents the mean±S.D. of three independent measurements. $^{*}p<0.05$, $^{**}p<0.01$; significantly different from control (DRV alone).

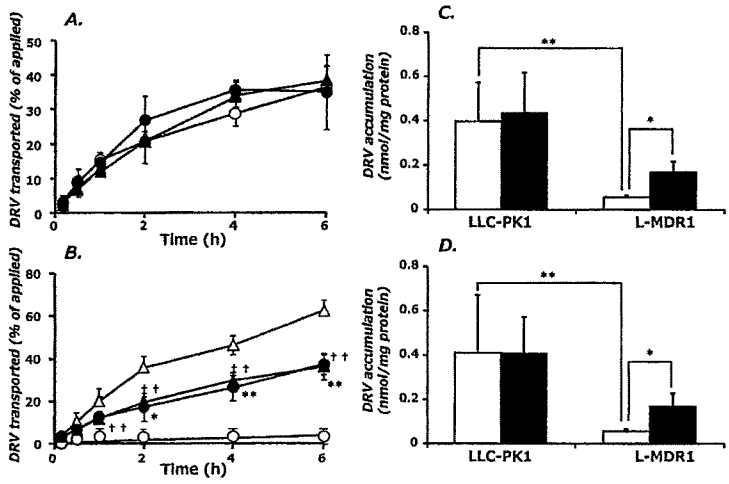

Fig. 3. Transepithelial Transport and Intracellular Accumulation of DRV in LLC-PK1 Cells and L-MDR1 Cells

Transport of DRV (10 μM) in the apical-to-basal direction (○, ●) and in the basal-to-apical direction (△, ▲) in the absence (control, open symbol) or presence (closed symbol) of cyclosporin A (10 μM) in LLC-PK1 (A) or L-MDR1 (B) cells. Each point represents the mean±S.D. of three independent measurements. $^{**}p<0.01$, $^{*}p<0.05$, significantly different from apical-to-basal transport without cyclosporin A. $^{\dagger\dagger}p<0.01$, significantly different from basal-to-apical transport without cyclosporin A. Intracellular accumulation of DRV in the absence (control, open column) and presence of cyclosporin A (closed column) 6 h after addition of DRV (10 μM) to the apical side (C) and basal side (D) of the monolayer. Each point represents the mean±S.D. of three independent measurements. $^{**}p<0.01$, significantly different from DRV accumulation in LLC-PK1 cells without cyclosporin A. $^{*}p<0.05$, significantly different from DRV accumulation in L-MDR1 cells without cyclosporin A.

lial Transport of DRV in LLC-PK1 and L-MDR1 Cells P-glycoprotein is an efflux pump responsible for limiting the oral bioavailability and tissue penetration of saquinavir.[25] In order to confirm the involvement of P-glycoprotein in DRV transport, we compared transepithelial transport of DRV in untransfected renal LLC-PK1 cells and ABCB1/MDR1 gene-transfected LLC-PK1 (L-MDR1) cells overexpressing P-glycoprotein in the apical membrane domain. As shown in Fig. 3A, there was no difference in the transport of DRV between the apical-to-basal and basal-to-apical directions in the LLC-PK1 cell monolayers. However, the basal-to-apical transport of DRV was much greater than the apical-to-basal transport in L-MDR1 cell monolayers. Furthermore, cyclosporin A markedly decreased the basal-to-apical transport and increased apical-to-basal transport of DRV in L-MDR1 cells (Fig. 3B). Figures 3C and D show the intracellular accumulation of DRV after incubation with the drug on either the apical or basal side of the monolayer in the presence and absence of cyclosporin A. In all cases, the accumulation of DRV was much lower in L-MDR1 cells in comparison to LLC-PK1 cells. Cyclosporin A significantly increased the accumulation of DRV from both sides of the monolayer. These findings suggest that transepithelial transport of DRV is stimulated *via* P-glycoprotein in L-MDR1 cells.

Inhibitory Effects of PIs on Transepithelial Transport of DRV in L-MDR1 Cells NFV markedly enhanced the apical-to-basal transport of DRV, but suppressed the basal-to-apical transport (Figs. 4A, 4B). RTV or SQV at a concentration of 50 μM significantly increased apical-to-basal DRV transport and decreased DRV transport in the opposite direction. Net secretory transport, evaluated as the ratio of basal-to-apical to apical-to-basal transport, showed NFV to have a potent inhibitory effect on P-glycoprotein-mediated transport of DRV when compared to RTV and SQV (Fig. 4C). RTV and SQV showed inhibitory effects on the net secretory transport of DRV at a concentration of 50 μM.

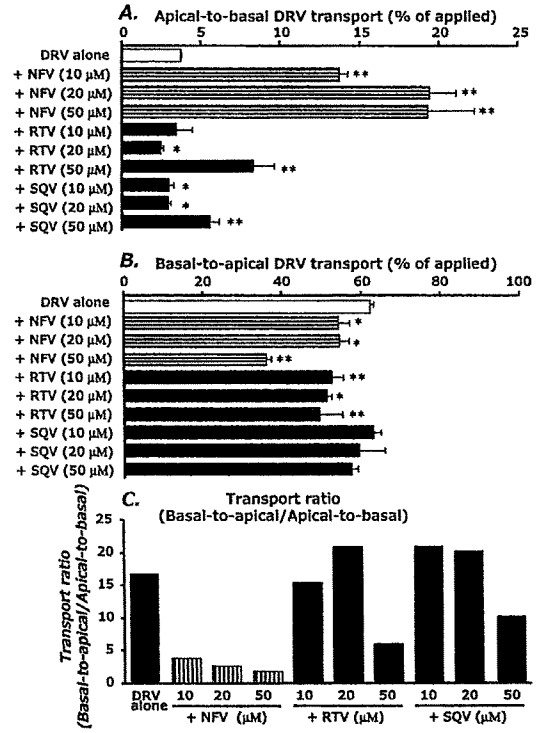

Fig. 4. Effect of PIs on the Transepithelial Transport of DRV in L-MDR1 Cells 6 h after Incubation with DRV

Transport of DRV (10 μM) in the apical-to-basal direction (A) or basal-to-apical direction (B). The transport ratio (basal-to-apical/apical-to-basal) is given in (C). Each point represents the mean±S.D. of three independent measurements. $^{**}p<0.01$, $^{*}p<0.05$, significantly different from control (DRV alone).

Inhibitory Effect of DRV on P-Glycoprotein-Mediated Calcein-AM Efflux In order to evaluate inhibitory effects of DRV on P-glycoprotein transport activity, calcein-AM ex-

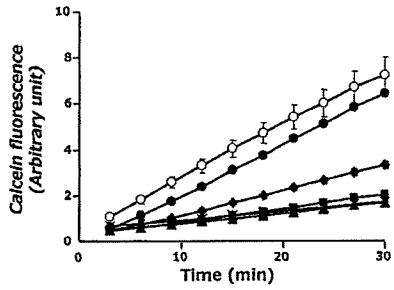

Fig. 5. The Effect of DRV on Intracellular Uptake of Calcein-AM in LLC-PK1 and L-MDR1 Cells Monolayers

LLC-PK1 cells without DRV (○), L-MDR1 cells without DRV (×), L-MDR1 cells with DRV at concentrations of 10 μM (▲), 25 μM (■), 50 μM (◆) and 100 μM (●). Each point represents the mean±S.D. of five independent measurements.

trusion test was performed using LLC-PK1 and L-MDR1 cells. As shown in Fig. 5, cellular accumulation of calcein was time dependent. Calcein accumulated much faster in LLC-PK1 cells than in L-MDR1 cells, confirming that calcein-AM was actively excluded in L-MDR1 cells by P-glycoprotein. RTV increased calcein accumulation in a dose-dependent manner in L-MDR1 cells, suggesting inhibition of P-glycoprotein activity. LLCmax of DRV was 121 μM and this potent inhibitory effect was comparable to that of RTV (LLCmax=111 μM).[20]

DISCUSSION

It has been reported that most of the currently available PIs are transport substrates of P-glycoprotein.[25,26] P-glycoprotein expressed in intestinal epithelial cells is thought to decrease absorption of orally administered PIs. Low levels of intestinal absorption together with CYP P450 activity are major factors in the first-pass effect of these drugs.[16,26] For example, it was reported that the area under the time-plasma concentration curves (*AUC*) after oral administration of SQV in *mdr1*-knockout mice was elevated five-fold compared to that of wild-type mice.[27] Moreover, Meaden *et al.* reported that P-glycoprotein expression levels in lymphocytes of patients coadministered with RTV and SQV were negatively correlated with the cellular accumulation of these PIs.[21] It was also suggested that P-glycoprotein expressed in the blood-brain barrier and blood-placenta barrier participate in the restricted distribution of indinavir, SQV, NFV or amprenavir into the brain and placenta, respectively.[28,29] Therefore, P-glycoprotein is thought to play a key role in the pharmacokinetics and therapeutic efficacy of most PIs. It was reported that DRV had a weak inhibitory effect (IC_{50}>100 μM) on P-glycoprotein expressed in *MDR1*-gene transfected Madin–Darby canine kidney (MDCK) cells.[30] However, it was not known whether DRV is recognized by P-glycoprotein as a transport substrate.

We explored transcellular transport of DRV using Caco-2 cells, which have been demonstrated to express ATP-binding cassette (ABC) transporter family members including ABCB11/P-glycoprotein, MRPs (ABCC2-6) and BCRP, OATP (SLCO) family members OATP-A and OATP-B, organic cation transporter OCT1 (SLC22A1), and organic anion transporter OAT2 (SLC22A7).[22,31—33] In the present study, typical P-glycoprotein inhibitors, cyclosporin A and verapamil, enhanced the apical-to-basal transport of DRV in Caco-2 cells, suggesting that P-glycoprotein mediates efflux transport of DRV in the apical membranes of Caco-2 cells. The ratio of basal-to-apical to apical-to-basal transport was approximately 2.2, indicating that net secretary transport of DRV is preferred in Caco-2 epithelial cells. Probenecid and MK571, nonspecific MRP inhibitors, also had significant but much weaker effects on the apical-to-basal transport of DRV in Caco-2 cells. Huisman *et al.* reported that indinavir, SQV and RTV were transported by MRP2, but not by MRP1 and MRP3.[34] Moreover, Williams *et al.* reported that SQV could be a substrate for P-glycoprotein, MRP1 and MRP2 with the transportability of P-glycoprotein>MRP2 MRP1.[35] Therefore, our results suggest that MRP2 could mediate, at least in part, the apical efflux of DRV in Caco-2 cells. Novobiocin, a typical BCRP inhibitor,[24] stimulated the basal-to-apical transport of DRV in Caco-2 cells. This finding suggests that BCRP is not involved in the transcellular transport of DRV, because BCRP is localized in the apical membranes of Caco-2 cells where it mediates efflux of substrates. However, we cannot exclude the possibility that unidentified novobiocin-sensitive transporter(s) expressed in the basolateral membranes of Caco-2 cells may also mediate the efflux transport of DRV. The OATP non-specific inhibitors, rifamycin SV and BSP,[32,33] showed weak but significant stimulatory effects on the apical-to-basal transport. Interestingly, this represents the opposite net direction of transport for DRV, suggesting a partial involvement of OATP-A and/or OATP-B in transcellular transport of this drug in Caco-2 cells. In the inhibition studies with glycylleucine and glycylsarcosine, we found no contribution of PEPT1 to apical DRV transport in Caco-2 cells. These findings suggest that P-glycoprotein mediates predominantly efflux transport of DRV in the apical membranes of Caco-2 cells, but other apical membrane-localized efflux transporters MRP2 and/or BCRP, and also OATP might be involved, at least in part, in transcellular transport of DRV.

The present work using L-MDR1 cells provides the first direct evidence that DRV is a transport substrate of P-glycoprotein. The inhibitory potency of DRV was comparable to that of RTV. In HIV therapy, the bioavailability of DRV (100 mg two times a day) is improved by oral coadministration with RTV (600 mg) *i.e.*, from 37% for DRV alone to 82% in combination with RTV.[15] It is generally thought that the boosting effect of RTV is due to the inhibition of oxidative metabolism in the intestine and liver by specifically targeting CYP3A4 activity.[15] Indeed, the apparent inhibition constant (K_i) of RTV for CYP3A4 and human hepatic microsomes were reported to be 0.10 μM and 0.17 μM, respectively, suggesting RTV is a potent inhibitor of CYP3A4.[36] However, our results demonstrate that the mechanisms of action of RTV in terms of improving the bioavailability of DRV involve inhibition of the efflux transport systems of the intestinal lumen in addition to the intestinal/hepatic metabolism. Further investigation is required in order to explore the relative contribution of these two mechanisms towards the improvement of oral bioavailability of DRV in clinical treatment.

In conclusion, the present study has revealed that DRV is a transport substrate of P-glycoprotein in Caco-2 cells and in *MDR1* gene-transfected renal LLC-PK1 cells. MRP, most

likely MRP2, was found to be partially involved in the apical efflux transport of DRV in Caco-2 cells. Furthermore, our results suggest RTV inhibits P-glycoprotein, thereby enhancing the apical-to-basal transport (*i.e.*, absorptive pathway) of DRV.

Acknowledgements This work was supported in part by a Grant-in-Aid for Scientific Research from the Japan Society for the Promotion of Science (JSPS) for Hideyuki Saito (KAKENHI 17390158) and Akinobu Hamada (KAKENHI 19590149).

REFERENCES

1) Bartlett J. A., Fath M. J., Demasi R., Hermes A., Quinn J., Mondou E., Rousseau F., *AIDS*, **20**, 2051—2064, (2006).
2) Piacenti F. J., *Pharmacotherapy*, **26**, 1111—1133 (2006).
3) Belmonte L., Baré P., de Bracco M. M., Ruibal-Ares B. H., *Curr. Med. Chem.*, **10**, 303—312 (2003).
4) Kozal M. J., Hullsiek K. H., Macarthur R. D., Berg-Wolf M., Peng G., Xiang Y., Baxter J. D., Uy J., Telzak E. E., Novak R. M., *HIV Clin. Trials*, **8**, 357—370 (2007).
5) Siliciano J. D., Siliciano R. F., *J. Antimicrob. Chemother.*, **54**, 6—9 (2004).
6) Barbaro G., *Am. J. Ther.*, **13**, 248—260 (2006).
7) Haugaard S. B., *Expert Opin. Drug Metab. Toxicol.*, **2**, 429—445 (2006).
8) Boyle B. A., *AIDS Read.*, **14**, 71—74 (2004).
9) Røge B. T., Barfod T. S., Kirk O., Katzenstein T. L., Obel N., Nielsen H., Pedersen C., Mathiesen L. R., Lundgren J. D., Gerstoft J., *HIV Med.*, **5**, 344—351 (2004).
10) Ghosh A. K., Sridhar P. R., Leshchenko S., Hussain A. K., Li J., Kovalevsky A. Y., Walters D. E., Wedekind J. E., Grum-Tokars V., Das D., Koh Y., Maeda K., Gatanaga H., Weber I. T., Mitsuya H., *J. Med. Chem.*, **49**, 5252—5261 (2006).
11) Koh Y., Matsumi S., Das D., Amano M., Davis D. A., Li J., Leschenko S., Baldridge A., Shioda T., Yarchoan R., Ghosh A. K., Mitsuya H., *J. Biol. Chem.*, **282**, 28709—28720 (2007).
12) Mitsuya H., Maeda K., Das D., Ghosh A. K., *Adv. Pharmacol.*, **56**, 169—197 (2008).
13) Clotet B., Bellos N., Molina J. M., Cooper D., Goffard J. C., Lazzarin A., Wöhrmann A., Katlama C., Wilkin T., Haubrich R., Cohen C., Farthing C., Jayaweera D., Markowitz M., Ruane P., Spinosa-Guzman S., Lefebvre E., *Lancet*, **369**, 1169—1178 (2007).
14) Boffito M., Winston A., Jackson A., Fletcher C., Pozniak A., Nelson M., Moyle G., Tolowinska I., Hoetelmans R., Miralles D., Gazzard B., *AIDS*, **21**, 1449—1455 (2007).
15) Rittweger M., Arastéh K., *Clin. Pharmacokinet.*, **46**, 739—756 (2007).
16) Benet L. Z., Izumi T., Zhang Y., Silverman J. A., Wacher V. J., *J. Controlled Release*, **62**, 25—31 (1999).
17) Lee C. G., Gottesman M. M., Cardarelli C. O., Ramachandra M., Jeang K. T., Ambudkar S. V., Pastan I., Dey S., *Biochemistry*, **37**, 3594—3601 (1998).
18) Saito H., Inui K., *Am. J. Physiol.*, **265**, G289—G294 (1993).
19) Hamada A., Miyano H., Watanabe H., Saito H., *J. Pharmacol. Exp. Ther.*, **307**, 824—828 (2003).
20) Shiraki N., Hamada A., Yasuda K., Fujii J., Arimori K., Nakano M., *Biol. Pharm. Bull.*, **23**, 1528—1531 (2000).
21) Meaden E. R., Hoggard P. G., Newton P., Jtjia J. F., Aldam D., Cornforth D., Lloyd J., Williams I., Back D. J., Khoo S. H., *J. Antimicrob. Chemother.*, **50**, 583—588 (2002).
22) Hirohashi T., Suzuki H., Chu X. Y., Tamai I., Tsuji A., Sugiyama Y., *J. Pharmacol. Exp. Ther.*, **292**, 265—270 (2000).
23) Vavricka S. R., Van Montfoort J., Ha H. R., Meier P. J., Fattinger K., *Hepatology*, **36**, 164—172 (2002).
24) Shiozawa K., Oka M., Soda H., Yoshikawa M., Ikegami Y., Tsurutani J., Nakatomi K., Nakamura Y., Doi S., Kitazaki T., Mizuta Y., Murase K., Yoshida H., Ross D. D., Kohno S., *Int. J. Cancer*, **108**, 146—151 (2004).
25) Jain R., Agarwal S., Majumdar S., Zhu X., Pal D., Mitra A. K., *Int. J. Pharm.*, **303**, 8—19 (2005).
26) Kim R. B., Fromm M. F., Wandel C., Leake B., Wood A. J., Roden D. M., Wilkinson G. R., *J. Clin. Invest.*, **101**, 289—294 (1998).
27) Park S., Sinko P. J., *J. Pharmacol. Exp. Ther.*, **312**, 1249—1256 (2005).
28) Anderson B. D., May M. J., Jordan S., Song L., Roberts M. J., Leggas M., *Drug Metab. Dispos.*, **34**, 653—659 (2006).
29) Salama N. N., Kelly E. J., Bui T., Ho R. J., *J. Pharm. Sci.*, **94**, 1216—1225 (2005).
30) Tong L., Phan T. K., Robinson K. L., Babusis D., Strab R., Bhoopathy S., Hidalgo I. J., Rhodes G. R., Ray A. S., *Antimicrob. Agents Chemother.*, **51**, 3498—3504 (2007).
31) Englund G., Rorsman F., Rönnblom A., Karlbom U., Lazorova L., Gråsjö J., Kindmark A., Artursson P., *Eur. J. Pharm. Sci.*, **29**, 269—277 (2006).
32) Sai Y., Kaneko Y., Ito S., Mitsuoka K., Kato Y., Tamai I., Artursson P., Tsuji A., *Drug Metab. Dispos.*, **34**, 1423—1431 (2006).
33) Seithel A., Karlsson J., Hilgendorf C., Björquist A., Ungell A. L., *Eur. J. Pharm. Sci.*, **28**, 291—299 (2006).
34) Huisman M. T., Smit J. W., Crommentuyn K. M., Zelcer N., Wiltshire H. R., Beijnen J. H., Schinkel A. H., *AIDS*, **16**, 2295—2301 (2002).
35) Williams G. C., Liu A., Knipp G., Sinko P. J., *Antimicrob. Agents Chemother.*, **46**, 3456—3462 (2002).
36) Ernest C. S., Hall S. D., Jones D. R., *J. Pharmacol. Exp. Ther.*, **312**, 583—591 (2005).

Journal of
Medicinal
Chemistry
Article

J. Med. Chem. 2009, 52, 7689–7705 7689
DOI: 10.1021/jm900695w

Design, Synthesis, Protein–Ligand X-ray Structure, and Biological Evaluation of a Series of Novel Macrocyclic Human Immunodeficiency Virus-1 Protease Inhibitors to Combat Drug Resistance†

Arun K. Ghosh,*[,‡] Sarang Kulkarni,[‡] David D. Anderson,[‡] Lin Hong,[§] Abigail Baldridge,[‡] Yuan-Fang Wang,[⊥] Alexander A. Chumanevich,[⊥] Andrey Y. Kovalevsky,[⊥] Yasushi Tojo,[#] Masayuki Amano,[#] Yasuhiro Koh,[#] Jordan Tang,[§,∥] Irene T. Weber,[⊥] and Hiroaki Mitsuya[#,▽]

[‡]*Departments of Chemistry and Medicinal Chemistry, Purdue University, West Lafayette, Indiana 47907,* [§]*Protein Studies Program, Oklahoma Medical Research Foundation, Oklahoma City, Oklahoma 73104,* [∥]*Department of Biochemistry and Molecular Biology, University of Oklahoma Health Science Center, Oklahoma City, Oklahoma 73104,* [⊥]*Department of Biology, Molecular Basis of Disease, Georgia State University, Atlanta, Georgia 30303,* [#]*Departments of Hematology and Infectious Diseases, Kumamoto University School of Medicine, Kumamoto 860-8556, Japan, and* [▽]*Experimental Retrovirology Section, HIV and AIDS Malignancy Branch, National Cancer Institute, Bethesda, Maryland 20892*

Received May 22, 2009

The structure-based design, synthesis, and biological evaluation of a series of nonpeptidic macrocyclic HIV protease inhibitors are described. The inhibitors are designed to effectively fill in the hydrophobic pocket in the S1′–S2′ subsites and retain all major hydrogen bonding interactions with the protein backbone similar to darunavir (**1**) or inhibitor **2**. The ring size, the effect of methyl substitution, and unsaturation within the macrocyclic ring structure were assessed. In general, cyclic inhibitors were significantly more potent than their acyclic homologues, saturated rings were less active than their unsaturated analogues and a preference for 10- and 13-membered macrocylic rings was revealed. The addition of methyl substituents resulted in a reduction of potency. Both inhibitors **14b** and **14c** exhibited marked enzyme inhibitory and antiviral activity, and they exerted potent activity against multidrug-resistant HIV-1 variants. Protein–ligand X-ray structures of inhibitors **2** and **14c** provided critical molecular insights into the ligand-binding site interactions.

Introduction

HIV/AIDS has become one of the major medical and humanitarian challenges in the 21st century.[1] Highly active antiretroviral therapy (HAART[a]), which combines protease inhibitors along with reverse-transcriptase inhibitors, is currently used to combat this pandemic. HAART therapy has resulted in a significant decline in the number of deaths due to HIV infection in the developed countries.[2] One of the major challenges still faced is the emergence of drug-resistant viral strains rendering the present drug regimens ineffective.[3] There is an urgent need for development of antiretroviral agents with minimal side effects and broad-spectrum activity for current and future management of HIV/AIDS.

Recently, our structure-based design of inhibitors maximizing interactions within the active site protease backbone led to the development of nonpeptide inhibitors (**1**–**2**) that have shown picomolar enzyme affinity and exceptional antiviral activity against both wild-type and drug-resistant HIV-1 strains.[4–6] The X-ray crystallographic studies revealed that the backbone conformation of mutant protease is minimally distorted compared to wild-type HIV-1 proteases. We, therefore, speculated that maximizing "backbone binding" may be an important design strategy to combat drug resistance.[7] Inhibitor **1** (darunavir, TMC-114) was recently approved by the FDA for the treatment of drug-resistant HIV strains.[8] More recently, it has been approved for all HIV/AIDS patients including pediatric AIDS patients.[9] The protein–ligand X-ray structure of darunavir and its analogue **2** (TMC-126) exhibited extensive hydrogen bonding interactions with the backbone atoms throughout the active site of the HIV-1 protease.[10,11]

In our continuing efforts toward the conceptual design of novel PIs, we now plan to design PIs with functionalities that interact with the protein backbone as well as introduce flexible macrocycles involving P1′–P2′ ligands for effective repacking due to side chain mutations. The notion of such macrocyclic design evolved from the observation that certain mutations lead to decreased van der Waals interactions and increased the size of the S1 hydrophobic pocket. The X-ray structure and modeling studies of PI (2*S*,2′*S*)-*N*,*N*′-((2*S*,3*R*,4*R*,5*S*)-3-hydroxy-4-methyl-1,6-diphenylhexane-2,5-diyl)bis(3-methyl-2-(3-methyl-3-(pyridin-2-ylmethyl)ureido)butanamide) (A-77003)[12] indicated that the V82A mutant results in decreased van der Waals interactions with the phenyl rings in both the S1 and S1′-subsites.[13] There was also evidence of repacking of inhibitor side chains and enzyme atoms in the S1-subsite. On the basis of this insight of enzyme flexibility in accommodating alternate packing, we planned to design flexible macrocycles between the P1′ side chain and the P2′ sulfonamide ring to fill in the S1′ and S2′-subsites.[13] In particular, we envisioned

†The PDB accession code for **2**-bound HIV-1 protease X-ray structure is 3I7E and **14c**-bound HIV-1 protease X-ray structure is 3I6O.

*To whom correspondence should be addressed. Phone: (765)-494-5323. Fax: (765)-496-1612. E-mail: akghosh@purdue.edu.

[a]Abbreviations: HIV, human immunodeficiency virus; bis-THF, bis-tetrahydrofuran; PI, protease inhibitor; HAART, highly active antiretroviral therapy; APV, amprenavir; DRV, darunavir; SQV, saquinavir; IDV, indinavir; LPV, lopinavir; DIAD, diisopropyl azodicarboxylate.

Published on Web 09/11/2009 pubs.acs.org/jmc

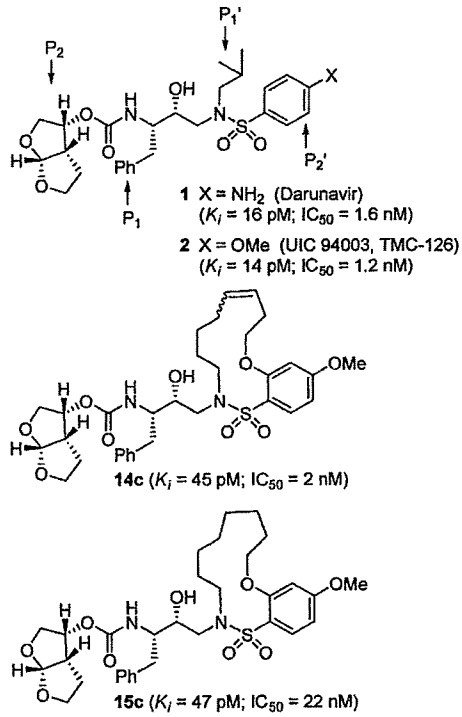

Figure 1. Structure of inhibitors **1**, **2**, **14c**, and **15c**.

Scheme 1. Synthesis of Sulfonyl Chlorides **7a–d**

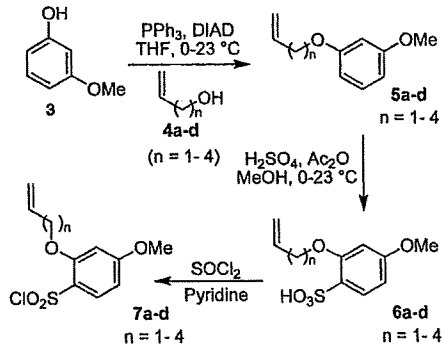

that 11–15-membered saturated and unsaturated macrocycles would effectively fill in the S1′–S2′ hydrophobic pocket of the enzyme active site while retaining all major interactions of PIs **1** and **2** with the protein backbone. Conceivably, such inhibitors will maintain potency against both wild-type and mutant strains. On the basis of this presumption, we designed a series of PIs that incorporated various macrocycles that could effectively fill in the enzyme active site. Herein we report the structure-based design, synthesis, and preliminary biological results of these macrocylic inhibitors. Among these compounds, **14b** and **14c** were the most potent, with both excellent enzyme inhibitory and antiviral activity. Both inhibitors exerted potent activity against multidrug-resistant HIV-1 variants. Furthermore, protein–ligand X-ray structures of inhibitors **2**- and **14c**-bound HIV-1 protease have revealed important insights regarding ligand-binding interactions (Figure 1).

Scheme 2. Synthesis of Compounds **13a–h**

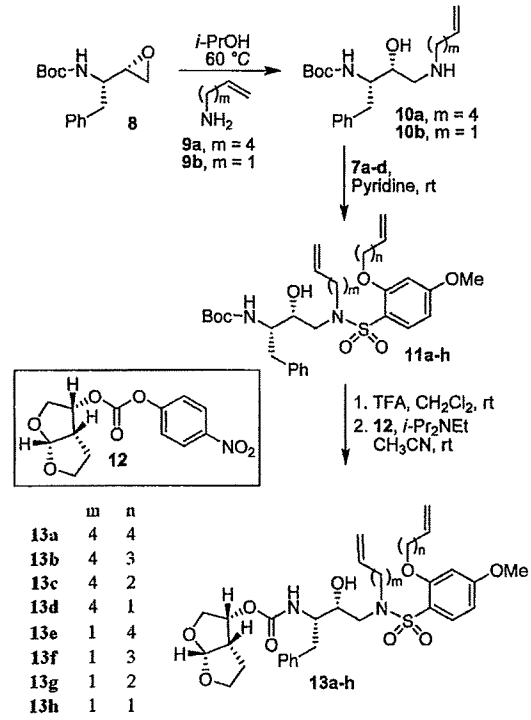

	m	n
13a	4	4
13b	4	3
13c	4	2
13d	4	1
13e	1	4
13f	1	3
13g	1	2
13h	1	1

Chemistry

The synthesis of sulfonyl chlorides **7a–d** is shown in Scheme 1. A Mitsunobu-type reaction between 3-methoxyphenol and alcohols **4a–d** in the presence of triphenylphosphine and diisopropyl azodicarboxylate (DIAD) afforded ethers **5a–d**.[14] Electrophilic aromatic substitution of ethers **5a–d** with acetic anhydride and concentrated sulfuric acid in methanol furnished a mixture of sulfonic acid regioisomers in a 1:1 ratio that were separated by flash chromatography to give **6a–d**. Structural confirmation of the isomers was determined by extensive 2D NMR experiments (NOESY and HMBC). Conversion to the sulfonyl chlorides **7a–d** was achieved by reaction of the sulfonic acids **6a–d** with thionyl chloride in the presence of pyridine.

The synthesis of compounds **13a–h** is outlined in Scheme 2. Nucleophilic attack of amines **9a** and **9b** on commercially available epoxide **8** in the presence of isopropyl alcohol gave hydroxy amines **10a** and **10b**. The conversion of amines **10a** and **10b** to the sulfonamides **11a–h** was realized by coupling with sulfonyl chlorides **7a–d** in the presence of pyridine. Removal of the Boc protecting group from sulfonamides **11a–h** using 30% trifluoroacetic acid in CH_2Cl_2 furnished the corresponding amines, which were then coupled with activated bis-THF[15] (**12**) to give acyclic inhibitors **13a–h**.

The acyclic compounds **13a–h** thus obtained were exposed to ring closing metathesis using Grubbs' first- or second-generation catalyst[16] (Scheme 3) to give the unsaturated macrocyclic inhibitors **14a–h**. Interestingly, larger ring sizes (15–13) gave a mixture of *E*/*Z* isomers, while in the case of smaller rings (12–9), the *Z* isomer was obtained exclusively. The *E* and *Z* isomers were isolated using reversed-phase HPLC and the stereochemistry established by 2D NMR

Scheme 3. Synthesis of Macrocyclic Inhibitors **14a–h** and **15a–h**

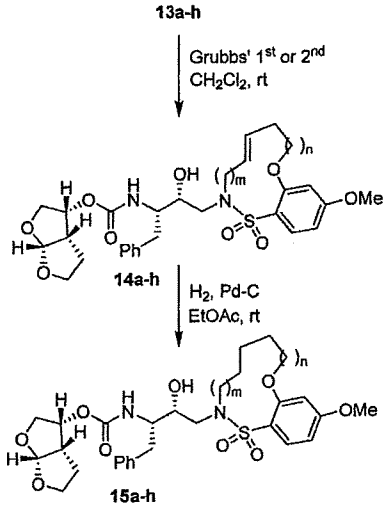

Scheme 4. Synthesis of Compounds **19a–c**

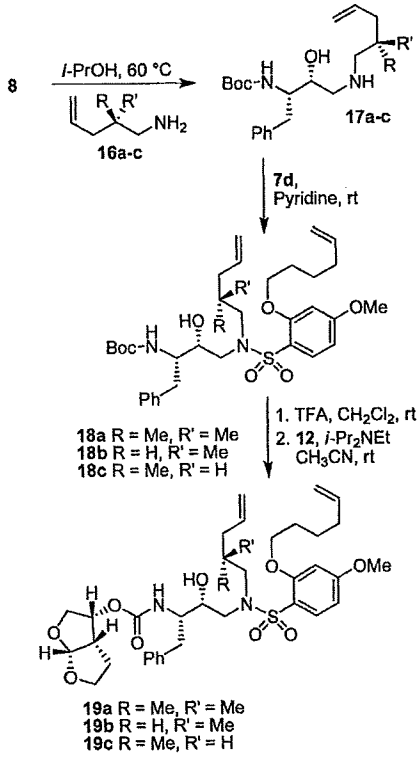

(COSY and NOESY) experiments, allowing their individual biological evaluation. The unsaturated compounds were subsequently reduced using hydrogen and 10% Pd–C as the catalyst to yield inhibitors **15a–h**.

A series of selectively methylated inhibitors were prepared in a similar fashion. Nucleophilic attack of amines **16a–c** on commercially available epoxide **8** gave hydroxy amines **17a–c** (Scheme 4). The conversion of amines **17a–c** to the sulfonamides **18a–c** was realized by coupling the amines with

Scheme 5. Synthesis of Macrocyclic Inhibitors **20a–c**, **21a–c**, and **22a–c**

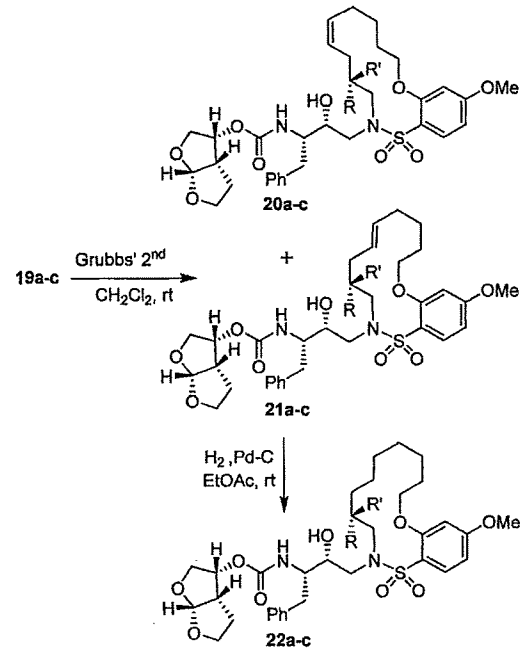

Table 1. Enzyme Inhibitory and Antiviral Activity of Inhibitors **13a–h**

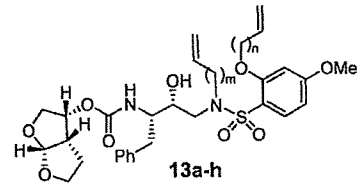

compd	m	n	K_i (nM)	IC_{50} (nM) [a]	ring size by RCM
13a	4	4	16.5 ± 0.5	> 1000	15
13b	4	3	11.5 ± 0.4	> 1000	14
13c	4	2	6.9 ± 0.1	ND	13
13d	4	1	10 ± 2	ND	12
13e	1	4	1.70 ± 0.07	270	12
13f	1	3	1.02 ± 0.08	290	11
13g	1	2	0.63 ± 0.01	ND	10
13h	1	1	0.10 ± 0.01	ND	9

[a] Human T-lymphoid cells, MT-2 cells (2×10^3), were exposed to HIV-1_{LAI} (100 $TCID_{50}$), cultured in the presence of each PI, and IC_{50} values were determined by using the MTT assay. The IC_{50} values of saquinavir (SQV) and amprenavir (APV) tested as reference agents were 16 and 27 nM, respectively. ND: not determined.

sulfonyl chloride **7d** in the presence of pyridine. Removal of the Boc protecting group from sulfonamides **18a–c** using 30% trifluoroacetic acid in CH_2Cl_2 furnished the corresponding amines, which were then coupled with the mixed carbonate of activated bis-THF[15] (**12**) to give acyclic inhibitors **19a–c**. A ring closing metathesis reaction using Grubbs' second-generation catalyst[16] (Scheme 5) provided a *E*/*Z* mixture of unsaturated macrocyclic inhibitors **20a–c** and **21a–c**, which were separated by reverse-phase HPLC and identified by 2-D NMR (COSY and NOESY). The unsaturated compounds